

University of Natural Resources and Life Sciences

Department for Agrobiotechnology, IFA-Tulln

Institute for Environmental Biotechnology



## Master Thesis

# Insights into laccase catalyzed polymerizations of lignosulfonate

Author: Valentina Bohinec, BSc  
**Master Program Biotechnology**

Supervisor: Univ.Prof. Dipl.-Ing. Dr.techn. Georg M. Gübitz  
**Institute for Environmental Biotechnology**

Co-supervisor: Dipl.-Ing. Karina Anna Stadler  
**Institute for Environmental Biotechnology**

**Tulln an der Donau, March 2019**

## Affidavit

I hereby declare that I am the sole author of this work. No assistance other than that which is permitted has been used. Ideas and quotes taken directly or indirectly from other sources are identified as such. This written work has not yet been submitted in any part.

Vienna, \_\_\_\_\_

Date

\_\_\_\_\_

Signature

## **Preamble**

I want to thank Univ.Prof. Dipl.-Ing. Dr.techn. Georg M. Gübitz and Dipl.-Ing. Karina Anna Stadler for the supervision of this master thesis. Moreover I want to thank Stephanie Supparitsch and Dipl.-Ing. Renate Weiß for the help and support through this work. I would also like to take the opportunity to express my gratitude towards my family, relatives and especially my boyfriend Renato Ivančič, who indirectly contributed toward the completion of my master thesis.

## Abstract

The biopolymer lignin, which is naturally found in plant cell walls, is the largest natural resource of aromatic compounds. As a side product from the pulp and paper industry, it is primarily used for energy generation. Only 1-2% of the produced lignin is used for the production of value-added products. The focus of this work was the valorization of lignin towards a stable and defined end product with high molecular weight, which could be used in paper coating formulations to replace fossil based latex as a binder.

Lignosulfonate polymers, originating from spent liquor out of pulp and paper industry, were purified and polymerized successfully with laccase. The used enzyme, *Myceliophthora thermophila* laccase (MtL), was characterized, resulting in a molecular weight (MW) of 64.6 kDa and a radius of gyration of 9.9 nm. Catalytic constants of MtL were determined at 23 °C with a 50 mM NaPi buffer pH 7.0 by using ABTS as model substrate. The Michaelis constant ( $K_M$ ) was determined to be 832.4  $\mu\text{M}$ , while the turnover number ( $k_{\text{cat}}$ ) was determined to be 192.4  $\text{s}^{-1}$ , resulting in a catalytic efficiency ( $k_{\text{cat}}/K_M$ ) of  $2.3 \times 10^5 \text{ s}^{-1} \text{ M}^{-1}$ . The highest enzymatic activity of MtL was observed between 60 and 65 °C.

The lignosulfonate (LS) polymerization process was monitored and confirmed by an increase in MW and viscosity, as well as a decrease in phenol and fluorescence content. Thermal treatment of the polymerized LS at 100 °C for 40 min or 110 °C for 20 min caused an inactivation of the enzyme, resulting in materials with average MWs of 300-1000 kDa and viscosities of 6-33 mPas depending on the LS concentration. Polymerized LS could be stored successfully at 21 °C for several weeks with a reasonable stability regarding MW and viscosity.

In conclusion, the thermal enzyme inactivation after laccase catalyzed polymerization showed promising outcomes. High molecular weight LS can be used for various applications as a green alternative to present solutions.

## Keywords

*Myceliophthora thermophila* laccase, polymerization, lignin, activity, inactivation, hydrodynamic radius, storage, thermal treatment, stability, molecular weight.

## Kurzfassung

Das Biopolymer Lignin, welches in Pflanzenzellwänden vorkommt, ist die größte natürliche Quelle von aromatischen Verbindungen. Lignin entsteht als Nebenprodukt in der Zellstoff- und Papierindustrie und wird hauptsächlich für Energieerzeugung verwendet. Nur 1-2% des produzierten Lignins werden zur Herstellung von Mehrwertprodukten verwendet. Im Mittelpunkt dieser Arbeit stand die Verwertung von Lignin. Das Ziel dieser Arbeit war es, ein stabiles und definiertes Endprodukt mit hohem Molekulargewicht zu erzeugen, welches für Papierbeschichtungsformulierungen verwendet werden und somit fossiles Latex als Bindemittel ersetzen könnte.

Lignosulfonat-Polymere aus der Dünnlauge der Zellstoff- und Papierindustrie wurden aufgereinigt und mit Laccasen erfolgreich polymerisiert. Das verwendete Enzym, *Myceliophthora thermophila* Laccase (MtL), wurde charakterisiert. Das Molekulargewicht betrug 64.6 kDa und der Gyrationradius 9.9 nm. Die katalytischen Konstanten von MtL wurden bei 23 °C mit einem 50 mM NaPi-Puffer pH 7.0 mit ABTS als Modells substrat bestimmt. Die Michaelis-Konstante ( $K_M$ ) wurde bei 832.4  $\mu\text{M}$  ermittelt, während die Wechselzahl ( $k_{\text{cat}}$ ) 192.4  $\text{s}^{-1}$  ergab. Die katalytische Effizienz ( $k_{\text{cat}} / K_M$ ) war demnach  $2.3 \times 10^5 \text{ s}^{-1} \text{ M}^{-1}$ . Die höchste enzymatische Aktivität von MtL wurde bei Temperaturen zwischen 60 und 65 °C beobachtet.

Während des Lignosulfonat (LS)-Polymerisationsprozesses konnte eine erfolgreiche Polymerisation durch eine Erhöhung des Molekulargewichts und der Viskosität, sowie durch eine Abnahme des Phenol- und Fluoreszenzgehaltes nachgewiesen werden. Die thermische Behandlung des polymerisierten LS bei 40 °C für 40 min oder 110 °C für 20 min führte zu der Inaktivierung des Enzyms. Abhängig von der LS-Konzentration, konnten dadurch Materialien mit einem durchschnittlichen Molekulargewicht zwischen 300 und 1000 kDa und Viskositäten zwischen 6 und 33 mPas erzeugt werden. Polymerisiertes LS konnte mit ausreichender Stabilität in Bezug auf das Molekulargewicht und die Viskosität für einige Wochen bei 21 °C gelagert werden.

Resultierend kann gesagt werden, dass die thermische Enzyminaktivierung nach der Polymerisation von LS durch Laccasen vielversprechende Ergebnisse liefert und hochmolekulares LS damit als grüne Alternative für verschiedene Bereiche anwendbar macht.

## Schlagworte

*Myceliophthora thermophila* laccase, Polymerisation, Lignin, Aktivität, Inaktivierung, hydrodynamischer Radius, Lagerung, thermische Behandlung, Stabilität, Molekulargewicht.

## Table of contents

List of figures .....	I
List of tables.....	II
List of abbreviations.....	IV
1 Introduction.....	1
1.1 Theoretical background.....	1
1.1.1 Lignin.....	1
1.1.2 Laccase.....	4
1.1.3 Enzyme inactivation .....	7
1.1.4 Analytical methods .....	7
1.2 Aims .....	12
2 Materials and Methods .....	13
2.1 Materials.....	13
2.1.1 Chemicals, Buffers and Solutions .....	13
2.1.2 Devices and Software .....	15
2.2 Methods .....	16
2.2.1 Enzyme purification and characterization .....	16
2.2.2 Lignosulfonate purification and characterization .....	21
2.2.3 Lignosulfonate polymerization.....	25
2.2.4 Lignosulfonate treatment.....	26
3 Results and Discussion .....	27
3.1 Characterization of laccase from <i>Myceliophthora thermophila</i> .....	27
3.1.1 Enzyme purification and size .....	27
3.1.2 Size and molecular weight of MtL .....	28
3.1.3 Enzymatic kinetics of MtL.....	29
3.1.4 Storage stability of MtL.....	31
3.1.5 Influence of temperatures on MtL activity .....	34
3.2 Lignosulfonate polymerizations.....	37

3.2.1	Properties of raw material .....	37
3.2.2	Monitoring of polymerizations .....	38
3.2.3	Influence of different temperatures on polymers and enzymatic activity.....	40
3.2.4	Storage stability of lignosulfonate polymers.....	44
4	Conclusion and Outlook .....	48
	References .....	52
	Appendix.....	55

## List of figures

Figure 1: Schematic view of a woody plant cell wall (Hüttermann, Mai and Kharazipour, 2001) .....	1
Figure 2: Structures of lignin and monolignols: p-coumaryl alcohol (H), coniferyl alcohol (G), and sinapyl alcohol (S) (Lupoi et al., 2015; Cannatelli and Ragauskas, 2016) .....	2
Figure 3: Copper centers of laccase: Type 1, Type 2, and Type 3 (Agrawal, Chaturvedi and Verma, 2018) .....	4
Figure 4: Schematic representation of reaction catalyzed by laccase (Agrawal, Chaturvedi and Verma, 2018) .....	6
Figure 5: Radius of gyration (hard sphere) and hydrodynamic radius (Nygaard et al., 2017) .....	10
Figure 6: Michaelis–Menten plot (Berg, Tymoczko and Stryer, 2002) .....	20
Figure 7: Lineweaver-Burk plot (Lineweaver-Burk plot, 2019) .....	20
Figure 8: Polymerization setup .....	25
Figure 9: SDS gel of ultrafiltrated MtL and fractions of purified MtL .....	27
Figure 10: MW and size determination with DLS instrument .....	28
Figure 11: SEC-MALLS chromatogram of purified MtL .....	28
Figure 12: Michaelis-Menten plot of purified MtL with ABTS as substrate .....	30
Figure 13: Storage stability of unpurified MtL at different temperatures .....	31
Figure 14: Storage stability of purified MtL at different temperatures .....	33
Figure 15: Activity of unpurified and purified MtL at temperatures from 35 to 70 °C .....	34
Figure 16: Size distributions of hydrodynamic radii over time after 90 °C heat treatment .....	35
Figure 17: Size distributions of hydrodynamic radii over time after 95 °C heat treatment .....	35
Figure 18: Size distributions of hydrodynamic radii over time after 99 °C heat treatment .....	36
Figure 19: Oxygen saturation during polymerization .....	38
Figure 20: Increase of molecular weight during polymerization .....	38
Figure 21: Fluorescence during polymerization .....	39
Figure 22: Phenol content during polymerization .....	40
Figure 23: Enzymatic activity during thermal treatments at 90, 100 and 110 °C .....	41
Figure 24: Viscosity decline during thermal treatment .....	42
Figure 25: Molecular weight decline during thermal treatment .....	42
Figure 26: Fluorescence during polymerization and after thermal treatment .....	43
Figure 27: Phenol content during polymerization and after thermal treatment .....	44
Figure 28: Enzymatic activity during different storing conditions .....	45
Figure 29: Viscosity of LS samples stored at different conditions .....	45
Figure 30: Molecular weights of lignosulfonate polymers stored at different conditions .....	46
Figure 31: Molecular weights of lignosulfonate polymers stored at different conditions .....	47

Figure 32: APPENDIX: BSA standard calibration curve .....	57
Figure 33: APPENDIX: Double reciprocal Lineweaver Burk plot of purified MtL .....	58

## List of tables

Table 1: List of chemicals .....	13
Table 2: List of materials.....	13
Table 3: List of buffers and solutions .....	14
Table 4: List of technical instruments, accessories and software.....	15
Table 5: Composition of MtL solution (unpurified) .....	16
Table 6: Settings of nanophotometer for determination of protein concentration .....	17
Table 7: DLS instrument settings.....	17
Table 8: Uniprot data of extracellular laccase lcc1 (Uniprot, 2019) .....	18
Table 9: Settings of Zetasizer for ZP measurement .....	24
Table 10: SDS gel sample legend and protein concentrations.....	27
Table 11: Summary of sizes and MWs for MtL.....	29
Table 12: Catalytic constants of purified MtL.....	29
Table 13: Catalytic constants from MtL with ABTS as substrate compared to values from literature .....	30
Table 14: Properties of the raw material.....	37
Table 15: The S/G ratio of the raw material.....	37
Table 16: Thermal stability coefficients of MtL in lignosulfonate solution .....	41
Table 17: Summary of storage stability .....	48
Table 18: APPENDIX: MW determination with DLS instrument .....	55
Table 19: APPENDIX: MW determination with MALLS .....	55
Table 20: APPENDIX: Theoretical MW computation with ProtParam .....	56
Table 21: APPENDIX: Bradford protein concentration of purified MtL .....	57
Table 22: APPENDIX: BSA standard calibration .....	57
Table 23: APPENDIX: Michaelis-Menten plot.....	57
Table 24: APPENDIX: Lineweaver–Burk plot.....	58
Table 25: APPENDIX: Storage stability data of unpurified MtL .....	59
Table 26: APPENDIX: Storage stability data of purified MtL .....	60
Table 27: APPENDIX: Temperatur optimum .....	61
Table 28: APPENDIX: Effect of high temperatures .....	61
Table 29: APPENDIX: Increase of molecular weight during polymerization.....	61
Table 30: APPENDIX: Fluorescence during polymerization and after thermal treatment .....	61
Table 31: APPENDIX: Phenol content during polymerization and after thermal treatment ...	62

Table 32: APPENDIX: Activity during thermal treatment .....	62
Table 33: APPENDIX: Thermal stability .....	62
Table 34: APPENDIX: Viscosity during thermal treatment .....	63
Table 35: APPENDIX: Molecular weight during thermal treatment .....	63
Table 36: APPENDIX: Activity during storage .....	64
Table 37: APPENDIX: Viscosity during storage .....	65
Table 38: APPENDIX: MW during storage .....	65

## List of abbreviations

ABTS	2,2'-azino-bis(3-ethylbenzothiazoline-6-sulphonic acid)
ATR	Attenuated total reflection
BSA	Bovine serum albumin
DLS	Dynamic light scattering
DS	Dry substance
EDL	Electric double layer
F	Fluorescence
FTIR	Fourier transform infrared
HPLC	High performance liquid chromatography
IR	Infrared
kat	katal
LMS	Laccase-mediator system
LS	Lignosulfonate
MALLS	Multi-angle laser light scattering
$M_n$	Number average molecular weight
MtL	<i>Myceliophthora thermophila</i> laccase
$M_w$	Weight average molecular weight
MW	Molecular weight
MWCO	Molecular weight cut-off
NaPi	Sodium phosphate
PDI	Polydispersity Index
RFU	Relative fluorescence units
$R_g$	Radius of gyration
$R_h$	Hydrodynamic radius
RI	Refractive index
rpm	Rounds per minute
SEC	Size exclusion chromatography
Tris-HCl	Tris(hydroxymethyl)aminomethane hydrochloride
UV/Vis	Ultraviolet/Visible
v/v	Volume per volume
w/v	Weight per volume
ZP	Zeta potential

# 1 Introduction

## 1.1 Theoretical background

### 1.1.1 Lignin

#### 1.1.1.1 Natural role of lignin

Lignin is the most abundant naturally occurring aromatic polymer. It comprises 20-35% of the dry weight of plant cell walls. The cell walls (figure 1) of woody plants are compounded materials made by in situ polymerization of a polyphenolic matrix (lignin) into a web of fibers (cellulose), a process that is catalyzed by polyphenoloxidases (laccases) or peroxidases. (Hüttermann, Mai and Kharazipour, 2001)

The heteropolymer confers strength and rigidity to plant cell walls and thus provides resistance against microbial attacks. It is responsible for the nutrient and water transport. (Beckham *et al.*, 2016) As a hydrophobic polymer it also serves as a barrier against water penetration (Christopher, Yao and Ji, 2014).

Figure 1 shows a woody plant cell wall at four different levels of magnification, namely a cross-section through a wood fiber (a) and through a part of the secondary cell wall with macrofibrils (b), a bundle of microfibrils (c) and micelle strands (d) and a cross-section through a micelle (e), indicating the ultrastructural composition: lignin, hemicellulose and cellulose. The interspace between the wood fibers (middle lamella), the macrofibrils, microfibrils and the micelles is filled with lignin.

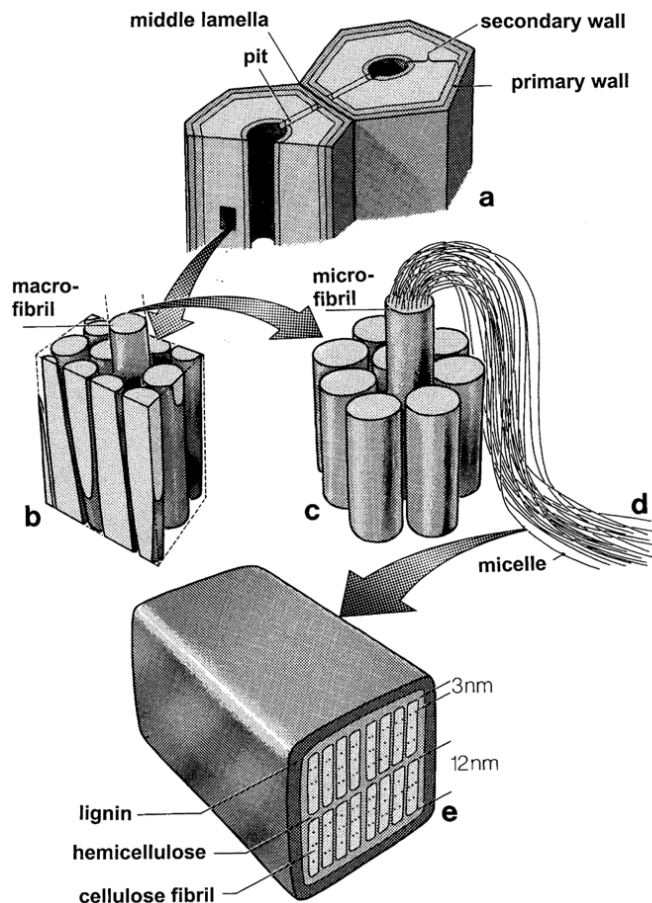


**Figure 1: Schematic view of a woody plant cell wall** (Hüttermann, Mai and Kharazipour, 2001)

Lignin biosynthesis proceeds through oxidative coupling reactions of radicals that lead to formation of a growing polymer linked by carbon-carbon and ether bonds. The resonance-

stabilized phenoxy radicals polymerize in a variety of monomer-oligomer and oligomer-oligomer coupling combinations through  $\beta$ -O-4,  $\alpha$ -O-4,  $\beta$ -5,  $\beta$ -1,  $\beta$ - $\beta$ , 5-5, dibenzodioxocin, and 4-O-5 linkages. (Christopher, Yao and Ji, 2014)

Lignin contains phenolic and nonphenolic subunits, which account for 10-30% and 70-90% of the polymer, respectively (Hilgers *et al.*, 2018).

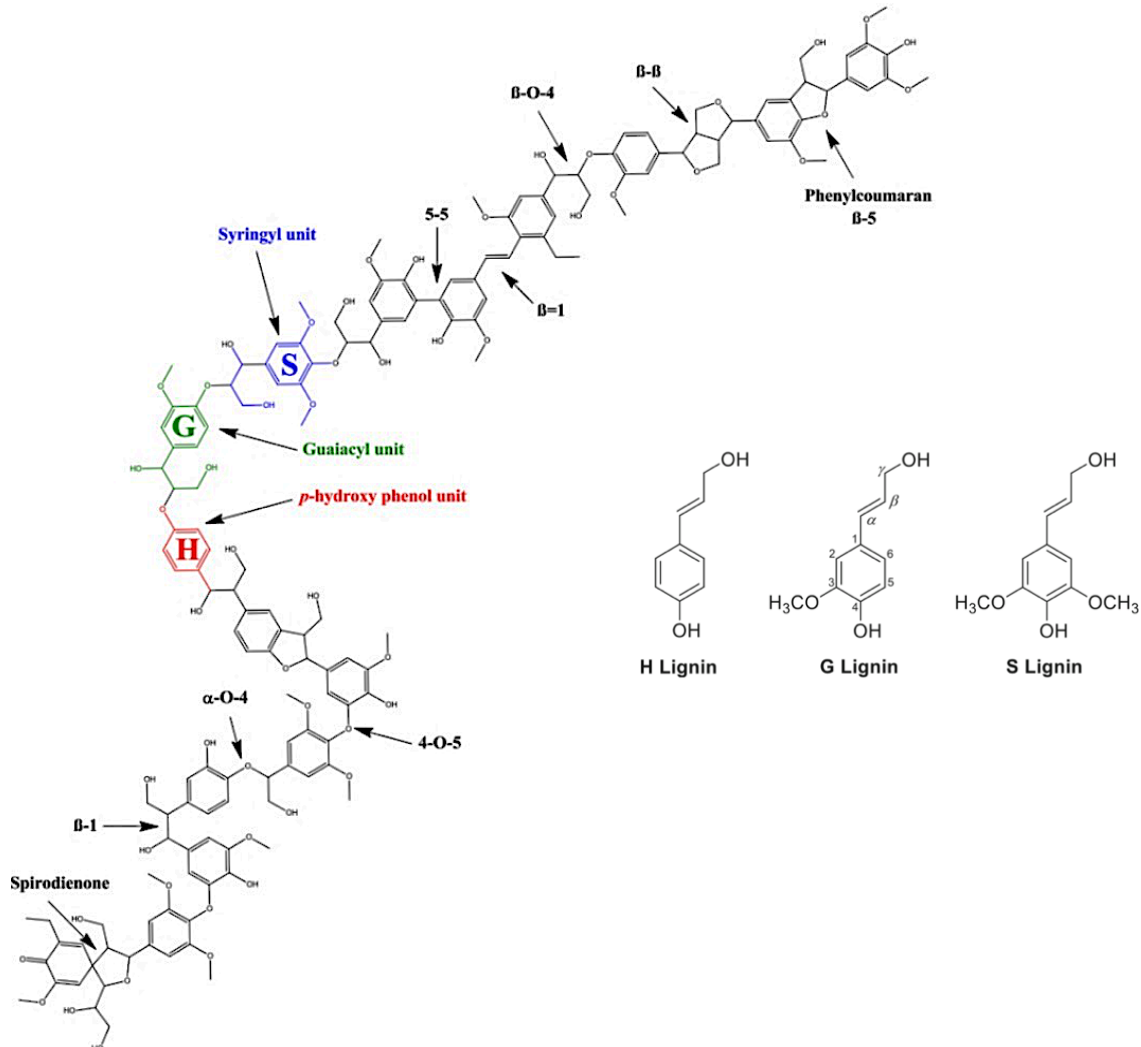


**Figure 2: Structures of lignin and monolignols: *p*-coumaryl alcohol (H), coniferyl alcohol (G), and sinapyl alcohol (S)** (Lupoi *et al.*, 2015; Cannatelli and Ragauskas, 2016)

The three primary units (figure 2): sinapyl (3,5-dimethoxy-4-hydroxycinnamyl), coniferyl (3-methoxy-4-hydroxycinnamyl) and *p*-coumaryl (4-hydroxycinnamyl) alcohols are linked through C-O and C-C bonds. These three monolignols or lignin precursors are also known as syringyl (S), guaiacyl (G), and *p*-hydroxy-phenyl (H) units, respectively. They differ in the number of methoxy groups that are attached to the aromatic moiety. Sinapyl alcohol has two methoxy groups, coniferyl alcohol has one methoxy group, and *p*-coumaryl alcohol has none. Based on the abundance of primary units, these polymers can be classified as G-type

(softwood lignin), GS-type (hardwood lignin), HGS-type (grass lignin) and HG-type (compression wood lignin). (Gillet *et al.*, 2017) Softwood lignin is built up mainly from G-units (up to 95%) with small amounts of H-units, whereas hardwood lignin has both, S- and G-units, in proportions from 1:1 to 1:3, with traces of H-units. Softwoods generally contain more lignin (25-35%) than hardwoods (20-25%). (Christopher, Yao and Ji, 2014)

### 1.1.1.2 Industrial lignins

The majority of lignin comes from pulp and paper industry, where it is produced during the delignification processes (Gillet *et al.*, 2017). Lignin demands partial degradation and extraction, yielding in the form of industrial lignin such as Kraft lignin (from the Kraft pulping process) or lignosulfonate (LS) (from sulfite pulping processes). Through the sulfite pulping process, lignin is extracted by the degradation of the lignin-carbohydrate complexes, and through (aqueous) solubilization by adding sulfonate groups to the aliphatic side chains of the phenylpropane units of lignin. (Gillgren, Hedenström and Jönsson, 2017) Due to the presence of the sulfonated groups, LS are anionically charged and water soluble (Aro and Fatehi, 2017).

The different conditions under which the pulping processes are carried out result in different structural properties of lignosulfonates. The typical pH-values of sulfite pulping processes range from 1 to 5, while the neutral sulfite semi-chemical pulping processes are carried out at pH 5-7. (Aro and Fatehi, 2017)

### 1.1.1.3 Applications

Today, lignin is primarily used for energy generation through combustion in pulping processes. Only 1-2% of the 50-70 million tons of lignin produced annually are used for the production of value-added products. (Aro and Fatehi, 2017)

The valorization of lignin is still underexploited but three main routes are considered relevant. The first is via lignin polymerization, which may result in properties beneficial for the application in binders and adhesives (Ortner *et al.*, 2018). Second, lignin depolymerization may lead to high-value low-molecular-weight aromatics. A third option is the functionalization of lignin via grafting of specific molecules onto lignin. A green alternative for all three routes is via biocatalysis; enzymes can be used for polymerization, depolymerization and also functionalization of lignin. In particular laccase is known for the key activities toward lignin. (Hilgers *et al.*, 2018)

The unique properties of LS make it possible to use it in a wide range of applications, such as animal feed, pesticides, surfactants, additives in oil drilling, stabilizers in colloidal suspensions,

as plasticizers in concrete admixtures, as dispersants, flocculants, metal adsorbents, dust suppressants and antioxidants, to name just a few. (Aro and Fatehi, 2017)

## 1.1.2 Laccase

### 1.1.2.1 Laccase diversity

Laccase is a copper-containing phenol oxidase, which can oxidize electron-rich substrates of phenolic and non-phenolic origin. The functions of laccases are diverse. They are involved in both lignin biosynthesis and lignin degradation, pigment formation in fungal spores, plant pathogenesis, and as fungal virulence factors, in iron metabolism and kernel browning processes in plants. (Christopher, Yao and Ji, 2014)

Laccases are found in plants, insects and bacteria, but are predominant in fungi (Alcalde, 2007). Fungal laccases are responsible for detoxification, fructification, sporulation, phytopathogenicity, and lignin degradation (Christopher, Yao and Ji, 2014). The most powerful laccases are produced by white-rot fungi and can have redox potentials up to 800 mV vs NHE (Hilgers *et al.*, 2018).

These multicopper proteins use molecular oxygen to oxidize a broad spectrum of organic compounds (Strong and Claus, 2011). The four copper centres inside the enzyme capture one type 1 Cu (T1), one type 2 Cu (T2) and a coupled binuclear type 3 (T3) Cu centre (figure 3).

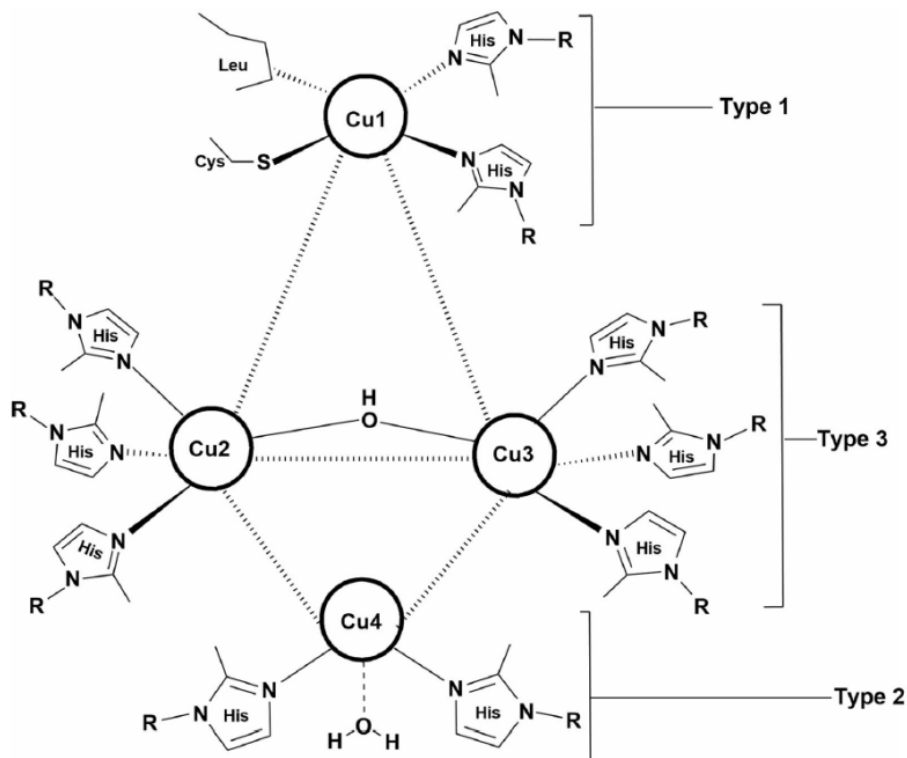


**Figure 3: Copper centers of laccase: Type 1, Type 2, and Type 3** (Agrawal, Chaturvedi and Verma, 2018)

The enzyme is able to oxidize phenolic systems by an outersphere electron transfer process that generates a radical cation, which generates a reactive phenoxy radical electron by fast deprotonation. The phenoxy radical intermediates, formed during this process, can further disproportionate or couple and consequently initiate lignin degradation. (Crestini *et al.*, 2010)

Laccase shows a high thermal resistance (stable at 60 °C), low substrate specificity and high oxidation rates that make this enzyme an ideal candidate for the development of efficient processes for lignin modification. (Crestini *et al.*, 2010)

One laccase used for lignin modification is synthesized by the thermophilic filamentous fungus *Myceliophthora thermophila*. This fungus, classified as an ascomycete, provides plant cell wall degrading enzymes with higher levels of specific activity and better stability at higher temperatures. *M. thermophila* grows in temperatures between 25 and 55 °C. The temperature optima for several enzymes from *M. thermophila* range from 50 to 70 °C. (Karnaouri *et al.*, 2014) *Myceliophthora thermophila* laccase (MtL) is a low redox potential laccase with a redox potential of 460 mV (Nugroho Prasetyo *et al.*, 2010).

#### 1.1.2.2 Substrates and mediators

Laccases are able to oxidize not only various aromatic compounds such as substituted phenols, aminophenols, polyphenols, o- and p-diphenols, polyamines, methoxy phenols, aryl diamines, aromatic amines, and thiols, but also some inorganic compounds such as iodine and ferrocyanide ions (Christopher, Yao and Ji, 2014).

With respect to laccase activity toward lignin, it is important to distinguish the phenolic and nonphenolic subunits in lignin. Laccases preferably act on phenolic compounds (Alcalde, 2007). The phenolic subunits can directly be oxidized by laccase, as the redox potentials of such subunits are sufficiently low. In contrast, the nonphenolic parts have redox potentials up to 1500 mV vs NHE and are, therefore, recalcitrant to oxidation by laccase alone. Nevertheless, when laccase is combined with a so-called mediator, oxidation of nonphenolic lignin structures is possible as well (figure 4). In such a laccase-mediator system (LMS), the mediator is first oxidized by the laccase, after which it can oxidize nonphenolic substrates via different mechanisms, such as electron transfer or radical hydrogen atom transfer. A LMS is required for the oxidation of the nonphenolic subunits in lignin and the phenolic subunits can be oxidized by laccase alone. (Hilgers *et al.*, 2018)

It is claimed that mediators enhance the laccase catalyzed lignin modification by two mechanisms:

- i) The mediators act as electron transfer agents between laccase and substrate, where the oxidized form of the mediator, i.e. after being catalytically oxidized by

laccase, diffuses away from the catalytic pocket and, due to its limited size, is capable of oxidizing substrates being inaccessible or too bulky for the laccase to oxidize directly.

- ii) The mediator expands the oxidizing capability towards oxidation of higher-redox potential non-phenolic subunits in lignin by introducing alternative reaction pathways for oxidation. (Munk, Andersen and Meyer, 2018)

Figure 4 shows different laccase catalyzed reactions. (a) represents a direct oxidation where the substrate is oxidized to the corresponding radical as a result of direct interaction and (b) represents in-direct oxidation where the substrate is oxidized in the presence of a mediator.

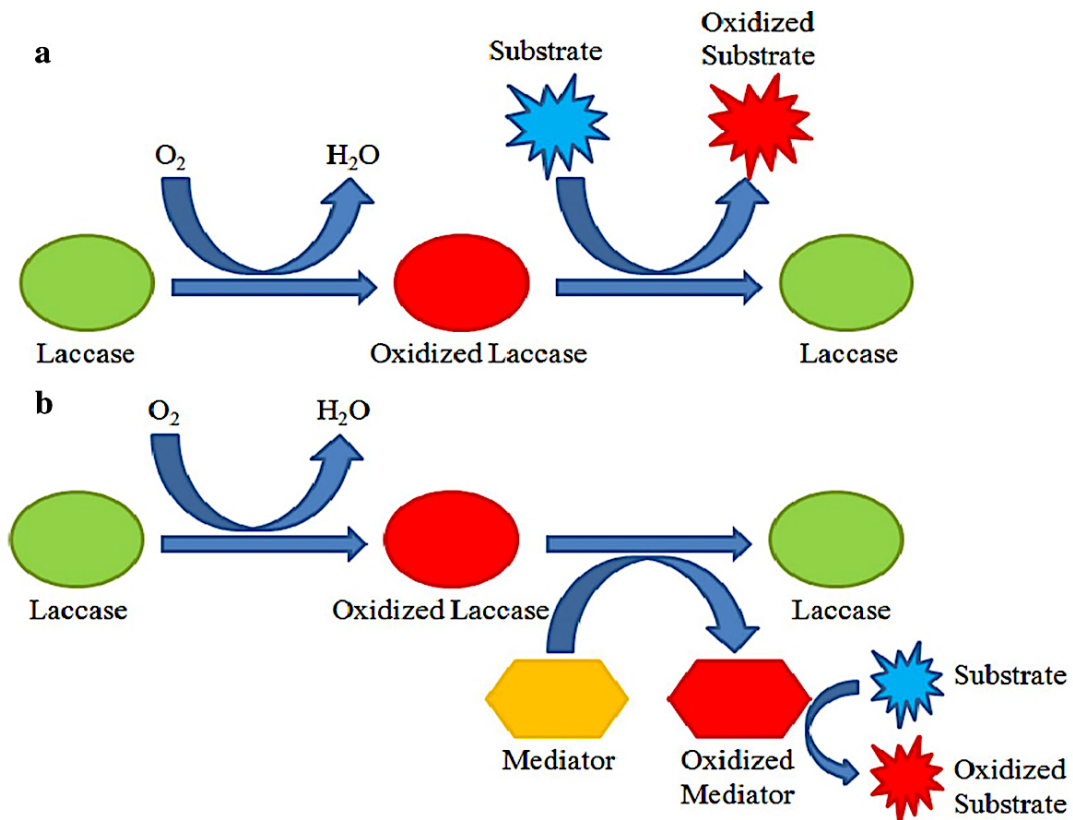


**Figure 4: Schematic representation of reaction catalyzed by laccase** (Agrawal, Chaturvedi and Verma, 2018)

Generally, all mediators are substrates of laccases. They are easily oxidized at the T1 site, in some cases producing very unstable and reactive cationic radicals which can in turn oxidize more complex substrates (Alcalde, 2007).

### 1.1.2.3 Lignosulfonate polymerization

Enzymatic polymerization is a sustainable and environmentally friendly option to increase the molecular weight (MW) of lignin. The recently discovered laccase lignin polymerization method from Ortner et al. leads, in the presence of an external oxygen supply and without the need of mediators, to extensive polymerized LS. MtL mediated polymerization leads to generation of

phenoxy radicals resulting in new ether and C-C, aryl-aryl or aryl-alkyl linkages and thus in higher MWs of LS. (Ortner *et al.*, 2018)

### 1.1.3 Enzyme inactivation

Laccases can be very strongly inhibited by various reagents. Small anions such as azide, halides, cyanide, thiocyanide, fluoride and hydroxide bind to the type 2 and type 3 Cu, resulting in the interruption of internal electron transfer and inhibition of activity. Other inhibitors include metal ions such as  $\text{Hg}^{2+}$ ,  $\text{Mg}^{2+}$ ,  $\text{Ca}^{2+}$ , and  $\text{Zn}^{2+}$  (Christopher, Yao and Ji, 2014), fatty acids, sulfhydryl reagents, hydroxyglycine, kojic acid, desferal and cationic quaternary ammonium detergents the reactions with which may involve amino acid residue modifications, conformational changes or Cu chelation. (Alcalde, 2007)

However, on an industrial scale a cheap and easy way of enzyme inactivation might be desired to stop enzymatic reactions. In order to avoid the addition of substances to the reaction mixture, protein denaturation by thermal treatment might be the method of choice.

### 1.1.4 Analytical methods

#### 1.1.4.1 Ultraviolet/visible spectroscopy

Ultraviolet/visible (UV/Vis) spectroscopy is a method, which measures the concentration of an analyte by absorbance in the UV/Vis spectral region. Absorbance is the process whereby monochromatic light is sent through a sample and the light intensity is diminished because molecules change from the ground state to an excited state. The principle is based on the Lambert-Beer law, which states that the absorbance of a solution is directly proportional to the concentration of the absorbing analyte and the path length. By keeping the path length constant, the concentration of an analyte can be determined. Absorbance is typically measured at the wavelength of maximum absorbance. (Măntele and Deniz, 2017)

Often colorimetric assays are used for the determination of protein concentrations. While some proteins can be quantified at 280 nm due to the presence of aromatic rings, others require a Bradford assay. The Bradford protein assay is based on an absorbance shift of the dye Coomassie Brilliant Blue G-250. The dye binds to the carboxyl group by Van der Waals forces and to the amino group through electrostatic interactions and thereby stabilizes the blue form of the Coomassie dye (anionic), while the unbound form is green (neutral) or red (cationic). (M. M. Bradford, 1976)

Another colorimetric assay for the determination of phenol groups was described by Blainski *et al.* (Blainski, Lopes and De Mello, 2013) The Folin-Ciocalteu (FC) assay is used to measure

the total concentration of phenolic hydroxyl groups that react with the FC reagent. A blue complex is formed by reduction of a phosphowolframate–phosphomolybdate complex. The amount of free phenolic groups is determined from a vanillin (4-hydroxy-3-methoxybenzaldehyde) standard curve. (Huber, Ortner, *et al.*, 2016)

#### 1.1.4.2 Fluorescence spectroscopy

Fluorescence spectroscopy relies on measurements of fluorescence spectra (Jeka *et al.*, 2010). Two basic types of spectra can be produced by conventional fluorescence spectrometers. In the emission spectrum, the wavelength of the exciting radiation is held constant (at an absorption wavelength of the analyte) and the spectral distribution of the emitted radiation is measured. In the excitation spectrum, the fluorescence signal is measured at a fixed wavelength of the emission selector as the wavelength of the exciting radiation is varied. An analyte can fluoresce only after it has absorbed radiation, and an excitation spectrum identifies the wavelengths of light that the analyte is able to absorb. (Gauglitz, 2003)

The fluorescence of lignin originates from several groups that are present in the lignin like phenylcoumaron, stilbene or carbonyl (Huber, Pellis, *et al.*, 2016).

#### 1.1.4.3 Fourier transform infrared spectroscopy

An infrared (IR) spectrometer produces IR light over a range of wavelengths and monitors the vibrations of molecules, which occur due to absorption of energy. Fourier transform (FT) is a mathematical operation that is used to convert the data to an absorbance/a transmittance over a frequency/wavelength form. FTIR can be operated in attenuated total reflection (ATR) mode, which is based on the attenuation effect of light when it is internally reflected between a material of high refractive index and a sample of low refractive index. Thereby, an evanescent wave of light penetrates into the sample. An IR spectrometer records light absorbed between  $4000\text{ cm}^{-1}$  and  $400\text{ cm}^{-1}$ . Frequencies with higher wavenumbers have more energy, while frequencies with lower wavenumbers have less energy. Bands between  $4000\text{ cm}^{-1}$  and  $1300\text{ cm}^{-1}$  indicate the presence of functional groups. The region between  $1300\text{ cm}^{-1}$  and  $400\text{ cm}^{-1}$  is called fingerprint region, since bands in this region are unique to each molecule. (Subramanian, Prabhakar and Rodriguez-Saona, 2011)

FTIR is a fast, label-free and nondestructive tool to identify the chemical structure of a sample. In lignin analysis it can be used to determine the S/G ratio, which is an important parameter that gives information about the lignin polymerization ability (Varanasi *et al.*, 2013). The S/G ratio is the ratio between syringyl-like lignin structures (S) and guaiacyl-like lignin structures (G) (Davison *et al.*, 2006). It is an indicator which type of wood, hard- or softwood, was used as raw material (Gillgren, Hedenström and Jönsson, 2017).

#### 1.1.4.4 High performance liquid chromatography - Size exclusion chromatography

Chromatography is a separation method for resolving a mixture of substances into its individual components. It is based on different retention times of these components, while they are travelling through a bed of resin particles. The solutes travel with different speeds depending on their affinity to a mobile or stationary phase.

Generally, high performance liquid chromatography (HPLC) instruments are designed for small-scale, high-resolution analytical applications. The resins are packed with small particles (2-5  $\mu\text{m}$ ), which allows running of HPLC systems with high pressure. (Jordan, 1996) Any analytes that can be dissolved, can be separated with different techniques, which are based on size, charge, solubility or biological activity.

Size exclusion chromatography or gel filtration separates macromolecules according to their hydrodynamic volume, which is defined by the Stokes radius. Size exclusion columns consist of porous polymer beads designed to have pores of different sizes. When a mobile phase is passed through the column, particles with small hydrodynamic volumes have a longer path length, as they equilibrate into the pores of the beads more often than those with large hydrodynamic volumes, which will result in their separation. (Kunji *et al.*, 2008)

HPLC systems are typically equipped with refractive index and UV detectors. For the determination of molar mass and the size of molecules it is also possible to add a multi-angle laser light scattering (MALLS) detector, where scattered light is measured in various angles.

#### 1.1.4.5 Dynamic and static light scattering

A particle in fluid that is not showing a trending movement like settling or floating, will randomly move due to multiple collisions with atoms or molecules (Brownian motion). If particles scatter an incident laser, the intensity of scattered light will fluctuate over time due to Brownian motion. In dynamic light scattering (DLS), these fluctuations are detected and analyzed with a correlator to get information about the moving particles. By assuming the spherical shape of the particles, the Stokes radius or hydrodynamic radius ( $R_h$ ) can be calculated (figure 5). (Podzimek, 2011) The  $R_h$  of a solute is the corresponding radius of a hard sphere that diffuses at the same rate as that solute.  $D_t$  is the translational diffusion coefficient. (Nygaard *et al.*, 2017)

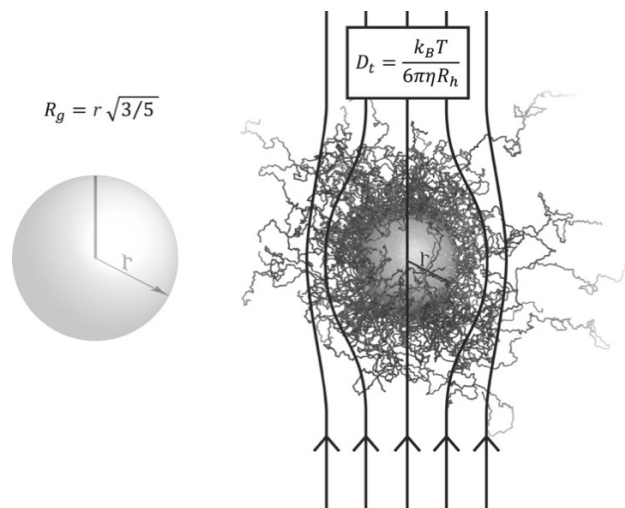


**Figure 5: Radius of gyration (hard sphere) and hydrodynamic radius** (Nygaard *et al.*, 2017)

In contrast to that, MALLS detection uses multiple fixed angles as part of a SEC setup (static light scattering) whereby the radius of gyration ( $R_g$ ) of an object can be calculated as the root mean-square distance between each point in the object and its center of mass. Thus, for a protein, it directly reports on the typical distance between an atom and the center of mass of the protein in the case of a solid sphere. (Nygaard *et al.*, 2017)

#### 1.1.4.6 Zeta potential

Most colloidal dispersions in aqueous solutions carry an electric charge. In this case, surrounding ions and molecules are attracted and form an electric double layer (EDL) around the charged particle. The EDL consists of an inner layer, which is predominantly made up of oppositely charged ions/molecules that are bound strongly (Stern layer), and a diffuse outer layer, which consists of positively and negatively charged ions/molecules. The diffuse layer is more dynamic, since it depends on various factors like pH, ionic strength, concentration etc. If the particle moves within an electric field (electrophoresis), ions/molecules within a hypothetical plane move with the particle, while those beyond this plane stay in the surrounding dispersant. This plane is called slipping plane and the potential at this boundary is the zeta potential (ZP).

The moving particles scatter a laser beam and the electrophoretic mobility can be calculated from the frequency shift, given by the difference in phase between the measured beat frequency and the reference frequency. The ZP can then be calculated from the electrophoretic mobility (see equations 11 and 12). (Bhattacharjee, 2016)

#### **1.1.4.7 Viscosity**

Viscosity is the property of fluids responsible for internal friction during flow (Doran, 2012). It is defined as the the ratio of shear stress to shear rate. If increasing (or decreasing) the shear stress increases (or decreases) the shear rate proportionally at a given temperature (such that the ratio does not change), the fluid is said to be a Newtonian fluid. If the shear rate does not increase proportionally with the shear stress, the fluid is said to be non-Newtonian fluid. Viscosity depends on temperature; the higher the temperature, the lower the viscosity. For reasonable accuracy when measuring viscosity, the temperature must be very carefully controlled. (Kenkel, 2003)

## 1.2 Aims

The main aim of this work was to get a defined and stable solution of high molecular weight lignosulfonate polymers that is suitable for application in paper coating formulations. The project aims to develop a green process that should be upscaled to industrial scale over the next few years. Therefore, process related decisions were made already in lab-scale in order to meet economical and technical criteria also on industrial scale. To get further insights into laccase catalyzed reactions and make the polymerization process controllable, the characterization and inactivation of the used enzyme *Myceliophthora thermophila* laccase was another goal.

## 2 Materials and Methods

### 2.1 Materials

#### 2.1.1 Chemicals, Buffers and Solutions

Table 1 shows the list of chemicals that were used during this work.

**Table 1: List of chemicals**

Chemicals	Supplier
Sodium phosphate dibasic dihydrate	Sigma-Aldrich (US)
Sodium phosphate monobasic monohydrate	Sigma-Aldrich (US)
Protein assay dye reagent concentrate	Bio Rad (Germany)
Sodium nitrate	Roth (Germany)
Sodium azide	Roth (Germany)
Folin & Cioacaltea's phenol reagent	Sigma-Aldrich (US)
Vanillin	Sigma Aldrich (US)
Protein standard, analy. standard, 200 mg/mL (BSA)	Sigma Aldrich (US)
ABTS (2,2'-azino-bis(3-ethylbenzothiazoline-6-sulphonic acid))	Roche (Germany)
2-Methoxyethanol, 99.8%	Sigma-Aldrich (US)
Trizma base	Sigma-Aldrich (US)
2-Mercaptoethanol	Sigma-Aldrich (US)
Laemmli 5× Concentrate	Sigma-Aldrich (US)
Protein Marker IV (pre-stained)	VWR (US)
Coomassie Brilliant blue G 250	Serva (Germany)
10x Tris/glycine/SDS running buffer (TGS)	Bio Rad (Germany)

Mg-Lignosulfonate was kindly provided by our company partner Sappi Gratkorn. All other reagents were of analytical grade and used as received if not otherwise specified.

Table 2 shows the list of used materials.

**Table 2: List of materials**

Materials	Specification	Supplier
Dialysis membrane	Standard RC Tubing Spectra/Por 3 (MWCO 3.5 kDa)	Spectrumlabs (US)
0.2 µm syringe filters	Chromafil Xtra PA-45/13	Macherey-Nagel (Germany)
Syringes	Norm-Ject Tuberkulin 1 mL	Henke Sass Wolf (Germany)
Filter Discs	Polyethersulfone membrane filters 15458 (0.1 µm)	Sartorius (Germany)

Size exclusion column	PD10 desalting column	GE Healthcare (US)
-----------------------	-----------------------	--------------------

Buffers and solutions as shown in table 3 were either freshly prepared or stored at 4 °C until use.

**Table 3: List of buffers and solutions**

Buffers and solutions	Preparation
50 mM sodium phosphate buffer, pH 7	Prepared with ultrapure water, pH was adjusted with sodium hydroxide and phosphoric acid
SEC eluent: 50 mM sodium nitrate + 3.1 mM sodium azide	Prepared with ultrapure water, filtrated (pore size 0.1 µm)
BSA standard: 1 mg/mL protein standard	Prepared with ultrapure water
Vanillin standard	Prepared with ultrapure water
FPLC binding and elution buffer: 20 mM Tris HCl, pH 7.6 20 mM Tris HCl, pH 7.6 + 1 M sodium chloride	Prepared with ultrapure water, pH was adjusted with hydrochloric acid and sodium hydroxide
TGS running buffer (1x)	10x TGS diluted with ultrapure water

## 2.1.2 Devices and Software

A list of technical instruments and the corresponding accessories are listed in table 4.

**Table 4: List of technical instruments, accessories and software**

Instruments	Specification	Supplier
Scale	MSX (SD EE)	Sartorius (Germany)
Freeze dryer	FreeZone 2.5 Plus	Labconco (US)
Plate reader	Tecan infinite M200 Pro	Tecan (Switzerland)
pH meter	SevenCompact S220	Mettler Toledo (Switzerland)
SEC	1260 Infinity	Agilent Technologies (US)
Guard column	PL aquagel-OH Guard, 8 µm, 7.5 mm, 50 mm (PL1149-1840)	
Column	PL aquagel-OH MIXED-H, 8 µm, 6-10000 kDa, >35000 p/m (PL1149-6800)	
SEC detectors		
RID	1260 Infinity	
MALLS	DAWN Heleos II	Wyatt Technology (Germany)
SEC Software	ASTRA 7 (Version 7.0.2.11)	
Nanophotometer	NP80	Implen (Germany)
Oxygen sensor	FireSting-O <sub>2</sub>	PyroScience (Germany)
Software	Firesting Logger (Firmware 2.30)	
Ultrafiltration system	Vivaflow 50 R	Sartorius (Germany)
Membrane	Hydrosart membrane MWCO 30 kDa	
Pump	Peristaltic pump MINIPULS Evolution	Gilson (US)
Rheometer	CVO 50	Bohlin Instruments (UK)
DLS instrument	DynaPro NanoStar	Wyatt Technology (Germany)
Cuvette	HE0136 MicroCuvette 1 µl ~DPN	
Software	Dynamics (Version 7.7.0.125)	
FT-IR spectrometer	Spectrum 100	Perkin Elmer (US)
Sample plate	Universal diamond ATR top-plate	
Software	Spectrum (Version 10.5.4)	
Nanophotometer	NP80	Implen (Germany)
Spectrophotometer	U-2900	Hitachi (US)
FPLC	ÄKTA pure	GE Healthcare (US)
Column	Anion exchange column HiTrap Q XL	
Electrophoresis		Biorad (US)
Chamber	Mini Protean II	
SDS gel	4–15% Mini-Protean TGX	

## 2.2 Methods

### 2.2.1 Enzyme purification and characterization

#### 2.2.1.1 Ultrafiltration: Laboratory crossflow filtration

The Novozym enzyme solution (unpurified MtL) as received from the supplier is composed of the ingredients stated in table 5.

**Table 5: Composition of MtL solution (unpurified)**

Ingredients	Approximate concentration in % (w/w)
Water	66
Propylene glycol	25
D-Sucrose/D-glucose	4
Myceliophthora thermophila Laccase	3
Glycine	2

For the first purification step an ultrafiltration system including a membrane with 30 kDa molecular weight cut-off (MWCO) was used. The liquid was circulated with the help of a peristaltic pump with 60 rpm until 10 volume exchanges with ultrapure water were completed.

#### 2.2.1.2 Ion exchange chromatography

The second purification step was done with anion exchange chromatography. The samples were prepared by using small size exclusion columns for buffer exchange into 20 mM Tris-HCl pH 7.6 (binding buffer). Afterwards, the anion exchange column was loaded with MtL binding buffer solution at a flow rate of 1 mL/min. Elution was performed with a 0-50% gradient of 20 mM Tris-HCl pH 7.6 with 1M NaCl (elution buffer). The eluted enzyme solution was collected in 12 fractions.

#### 2.2.1.3 Protein concentration

##### 2.2.1.3.1 Bradford protein assay

To determine the protein concentration of the purified laccase solution, a Bradford assay was carried out as suggested by the supplier. For the calibration curve, bovine serum albumin (BSA) standards from 0.05 to 0.5 mg/mL were prepared with ultrapure water. 10  $\mu$ L of each standard and accordingly diluted samples were pipetted into 96-well plates and 200  $\mu$ L of diluted dye reagent was added to each well. Samples were shaken at 300 rpm at 21 °C for 5 min and the absorbance was measured at 595 nm. All experiments were carried out in triplicates. The blank contained ultrapure water instead of lacasse and was treated like the

sample. The protein concentration was calculated via the linear equation of the BSA standard curve.

### 2.2.1.3.2 Nanophotometer

The protein concentration was also determined with a nanophotometer. The absorbance was measured at 280 nm with the predefined settings of BSA. Samples were diluted in ultrapure water and measured in triplicates. Ultrapure water was used as blank.

**Table 6: Settings of nanophotometer for determination of protein concentration**

Protein type	Volume [μL]	Pathlength [mm]	Extinction coefficient $\epsilon_{\text{prot}}$ [g cm L <sup>-1</sup> ]	Molar extinction coefficient [M <sup>-1</sup> cm <sup>-1</sup> ]	Background correction
BSA	1-2	Automatic change	1.5	44289	on

The protein concentration was calculated according to equation 1.

$$(A_{280} - A_{320}) = c * \epsilon_{\text{prot}} * d * DF$$

*Equation 1: Lambert Beer's Law*

$A_{280}$  ... Absorbance at 280 nm

$A_{320}$  ... Absorbance at 320 nm

c ..... Concentration

$\epsilon_{\text{prot}}$  ... Extinction coefficient

d ..... Pathlength

DF .... Dilution factor

### 2.2.1.4 Size determination

#### 2.2.1.4.1 Light scattering

For the determination of the radius of MtL two LS systems were used; a cuvette based DLS instrument and a MALLS detector attached to SEC.

Prior to measurements in the cuvette based DLS instrument 500 μL aliquots of purified MtL were incubated for 10 min at 21, 90, 95 and 99 °C. Afterwards 2 μL of each sample was transferred into a quartz cuvette and the measurement was started with the settings stated in table 7.

**Table 7: DLS instrument settings**

Solvent	Sample	Acquisitions	Acquisition time
Water (RI 1.333)	MW-R, Model: globular protein	20	2 s

Due to residual impurities in the samples, which interfered with the measurement, some runs had to be excluded from the data pool. For sample analysis the D10 value was used; It defines the radius/diameter that contains 10% of the cumulative distribution. The molecular weight (MW) could only be determined from samples that were incubated at only 21 °C (active enzyme). For analysis of heat treated samples, the size distribution curves were compared to D10 radii.

The  $R_h$  could be calculated by the Stokes-Einstein equation (see equation 2) from the diffusion coefficient, which was determined from the measured intensity fluctuations.

$$R_h = kT / 6\pi\eta D$$

*Equation 2: Stokes-Einstein equation*

- $R_h$  .... Hydrodynamic radius
- $k$  ..... Boltzman's constant
- $T$  ..... Absolute temperature
- $\eta$  ..... Solvent viscosity
- $D$  ..... Translational diffusion coefficient

For the second approach to determine the size of MtL, a MALLS detector that was connected to SEC was used (see chapter 2.2.2.5).

#### 2.2.1.4.2 Protparam tool

The ProtParam tool was used for the computation of MW based on the sequence of extracellular laccase lcc1 from *Myceliophthora thermophila* as summarized in table 8.

**Table 8: Uniprot data of extracellular laccase lcc1** (Uniprot, 2019)

<b>Gene name:</b>	lcc1 (MYCTH_51627)
<b>Protein name:</b>	Extracellular laccase (UniProtKB/TrEMBL G2QG31_MYCTT)
<b>Organism:</b>	<i>Myceliophthora thermophila</i> (strain ATCC 42464)

Since the sequence of lcc1 contains also a signal peptide, the MW of this signal peptide was subtracted to obtain the actual MW of the enzyme (see appendix table 21).

#### 2.2.1.4.3 Sodium dodecyl sulfate gel electrophoresis

To determine the purity and the MW of enzyme fractions after anion exchange chromatography of laccase, a SDS-PAGE was carried out. The gel run was performed in an electrophoresis chamber filled with TGS running buffer (1x). Enzyme and Laemmli buffer (2x) in ratio 1:1 were heated for 10 min at 99 °C. 15  $\mu$ L of the denatured sample mixture and 5  $\mu$ L protein marker IV were loaded on a polyacrylamide gel with 4-15% gel percentage. The electrophoresis was performed with 150-200V for 30-60 min. Afterwards, the gel was stained with brilliant blue for 20 min and destained with destaining solution for 30 min.

### 2.2.1.5 ABTS activity assay

For the determination of laccase activity, an ABTS assay was performed. The enzyme solution was diluted accordingly (1:30000) in 50 mM sodium phosphate (NaPi) buffer pH 7. For the measurement 170  $\mu$ L enzyme was added to 50  $\mu$ L of 10 mM 2,2'-azino-bis(3-ethylbenzothiazoline-6-sulphonic acid (ABTS) and measured immediately in a 96 well plate. 170  $\mu$ L of NaPi buffer with 50  $\mu$ L of 10 mM ABTS were used as blank. The absorbance was monitored at 420 nm. The activity was calculated in katal (kat) and corresponds to the amount of laccase converting 1 mol of ABTS per second. All experiments were carried out in triplicates. (Huber, Pellis, *et al.*, 2016)

The laccase activity was calculated according to following equation 3:

$$a = (k * DF * V_{total}) / (V_{enzyme} * \epsilon_{420} * d) \quad \text{Equation 3: Enzymatic activity}$$

- a ..... Enzymatic activity
- k ..... Slope
- $V_{total}$  ..... Volume total
- $V_{enzyme}$  ... Volume enzyme solution
- $\epsilon_{420}$  ..... Extinction coefficient
- d ..... Pathlength
- DF ..... Dilution factor enzyme solution

### 2.2.1.6 Activity maximum with varying temperature

To determine at which temperature the lacasse is most active, ABTS activity assays (see chapter 2.2.1.5) were carried out at different temperatures, ranging from 35 to 70 °C. For an optimal result, NaPi buffer pH 7 was incubated at the desired temperatures, before it was used for enzyme dilution. 850  $\mu$ L of the diluted lacasse were added to 250  $\mu$ L 10 mM ABTS and measured immediately at 420 nm. The measured blank contained NaPi buffer pH 7 instead of enzyme and was treated like the sample. The experiment was carried out in triplicates. The activity was calculated according to equation 3.

### 2.2.1.7 Kinetics of *Myceliophthora thermophila* laccase

In order to determine the maximal rate ( $v_{max}$ ) and the Michaelis-Menten constant ( $K_M$ ) of Mtl, the activity was measured at ABTS concentrations ranging from 0.1 to 40 mM at 21 °C. The experiment was carried out in triplicates. Activity determination was carried out as described in chapter 2.2.1.5.  $v_{max}$  and  $K_M$  were calculated from the linear equation obtained from the Lineweaver-Burk plot (see figure 7) according to equation 4 (see figure 6). The molarity of enzyme was calculated from the protein concentration obtained by the Bradford assay (see chapter 2.2.1.3.1) and the MW obtained from MALLS detection (see chapter 2.2.1.4.1).

$$k_{cat} = v_{max} / E$$

**Equation 4: Catalytic constant**

- $k_{cat}$  ... Catalytic constant
- $v$  ..... Reaction rate
- $E$  ..... Enzyme concentration

The maximal rate,  $v_{max}$ , is attained when the catalytic sites on the enzyme are saturated with substrate. The  $K_M$  value is equal to the substrate concentration at which the reaction rate is half  $v_{max}$ . The turnover number ( $k_{cat}$ ) is the number of substrate molecules converted into product by an enzyme molecule in a unit time when the enzyme is fully saturated with substrate. (Berg, Tymoczko and Stryer, 2002)

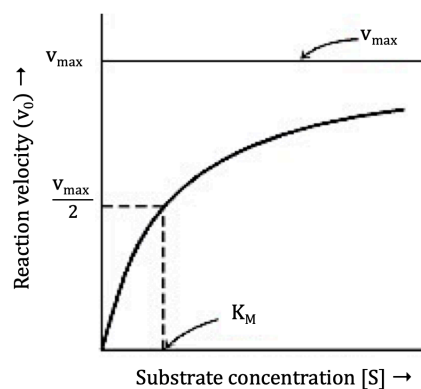


**Figure 6: Michaelis–Menten plot** (Berg, Tymoczko and Stryer, 2002)

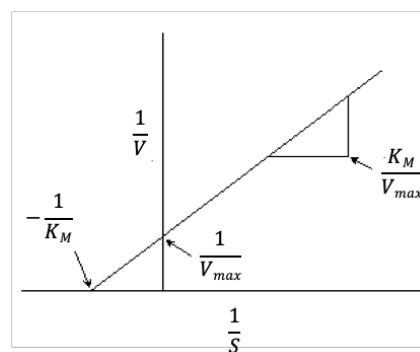


**Figure 7: Lineweaver-Burk plot** (Lineweaver-Burk plot, 2019)

### 2.2.1.8 Laccase storage stability

To determine the optimal storage conditions for laccase, aliquots of enzyme were stored at -80, -20, +4 and +21 °C, either 1:100 diluted in ultrapure water, 1:100 diluted in 50 mM NaPi buffer pH 7 or undiluted. The experiment was performed for purified and unpurified MtL. Activity assays were performed every few days up to 112 days (see chapter 2.2.1.5).

### **2.2.1.9 Oxygen monitoring**

The saturation of oxygen in liquids was measured with immobilized oxygen sensor spots in glass vessels. The sensor calibration (2-point calibration) for oxygen monitoring was done with atmospheric air (100%) and pure nitrogen (0%). The oxygen saturation was measured continuously during the polymerization process of lignosulfonates (see chapter 2.2.3.2). For data presentation, the axis for oxygen saturation was normalized to 100%.

## **2.2.2 Lignosulfonate purification and characterization**

### **2.2.2.1 Pretreatment of lignosulfonate solution**

The Mg-lignosulfonate that was used for this work originated from spent liquor out of a sulfite pulping process. The spent liquor was diafiltrated with a 5 nm membrane by our company partner Sappi Gratkorn. Further the lignin solution was dried at 60-70 °C for several days, grounded to powder and stored at 21 °C until use.

### **2.2.2.2 Dialysis**

Dialysis was used for the removal of salts from the lignosulfonate solution (only for characterization). 50 mL of 10% DS lignosulfonate was dialyzed against ultrapure water in a dialysis membrane with a MWCO of 3.5 kDa. Ultrapure water exchange was done every hour during the first 6 h and every few hours afterwards for 24 h.

### **2.2.2.3 Phenol content**

20 µL lignin diluted in ultrapure water (1:50), 60 µL FC-reagent and 600 µL pure water were mixed and incubated for 5 min at 21 °C. Afterwards, 200 µL sodium carbonate 20% (w/v) and 120 µL ultrapure water were added. The samples were incubated for 2 h at 800 rpm at 21 °C. After incubation, 200 µL of sample was transferred into a 96-well plate and the absorbance was measured at 760 nm. Prepared vanillin standards from 0.05 to 1 mg/mL were treated as the diluted lignin sample. The blank contained ultrapure water instead of lignin and was treated like the sample. The experiment was done in triplicates. (Ortner *et al.*, 2015)

### **2.2.2.4 Fluorescence of lignin**

For the measurement of fluorescent intensity, 100 µL lignin diluted in ultrapure water (1:5000) was mixed with 120 µL of 2:1 water/methoxyethanol (v/v) solution in a black 96-well plate. The sample was excited at 355 nm and the emitted light was measured at 400 nm. The blank contained ultrapure water instead of lignin and was treated like the sample. All measurements were done in triplicates. (Ortner *et al.*, 2015)

### **2.2.2.5 Fourier transform infrared spectroscopy**

FTIR spectra of freeze dried lignosulfonate were recorded to identify differences in their chemical profiles and to calculate the S/G ratio.

For each FTIR spectrum, dried sample was placed on the ATR sample plate and 30 scans were taken in a range of 600 to 4000  $\text{cm}^{-1}$  with a resolution of 4  $\text{cm}^{-1}$ . Normalization between 930 and 1070  $\text{cm}^{-1}$  and baseline correction was done.

### **2.2.2.6 Size exclusion chromatography with multi-angle laser light scattering**

A combination of SEC with RI-detector and MALLS detector was used to determine the MW of LS polymers and MtL. The samples were diluted with 50 mM sodium nitrate with 3.1 mM sodium azide (eluent) to a concentration of 1 mg/mL and filtrated through a 0.2  $\mu\text{m}$  syringe filter. The sample runs were performed at a flow rate of 0.3 mL/min. The loaded sample volume was 100  $\mu\text{L}$ . 1 mg/mL BSA standards were used for detector normalization, peak alignment of RI- and MALLS-signal, correction of band broadening and therefore calculation of the calibration coefficient.

The light scattering intensity is proportional to the concentration, the molecular weight and the refractive index increment. Since the concentration is known from RI detection and the  $\text{dn}/\text{dc}$  value can be determined for each substance specifically, the molecular weight can be determined according to equation 5. In this case, a weight average molecular weight ( $M_w$ ) was used for analysis (see equation 6).

$$I_s(\theta) \propto c * MW * (dn/dc)^2$$

*Equation 5: Light scattering equation*

$I_s$  ..... Scattering intensity at a specific angle

$C$  ..... Concentration

$MW$  ..... Molecular weight

$Dn/dc$  ... Refractive index increment

$$M_w = \sum (c_i * MW_i) / \sum c_i$$

*Equation 6: Weight average molecular weight*

$M_w$  ..... Weight average molecular weight

$c_i$  ..... Concentration

$MW_i$  ..... Molecular weight

The radius of gyration is calculated from the mass distribution around the center of the mass, weighted by the square of the distance from the center of the mass as described in equation 7:

$$(r_j^2)_z = \sum (c_i * M_i * (r_j^2)_i) / \sum c_i * M_i$$

*Equation 7: Radius of gyration/RMS radius*

$(r_j^2)_z$  ..... Mean square radius

The polydispersity index (PDI) represents the quotient of  $M_w$  and number average MW ( $M_n$ ) (see equation 8). For monodisperse samples the PDI is 1.00.

$$PDI = M_w / M_n$$

*Equation 8: Polydispersity index*

$M_w$  ... Weight average MW

$M_n$  .... Number average MW

### 2.2.2.7 Freeze drying

30 mL of sample were stored at -80 °C in 50 mL falcon tubes and sealed with perforated parafilm and stored at -80 °C until freeze drying. Freeze drying was performed at 21 °C, at 0.1 mbar for 2-3 days.

### 2.2.2.8 Viscosity

The viscosity of 1200  $\mu$ L lignin sample was determined with a 40 mm conical plate with 4° inclination at a constant temperature of 20°C and a constant shear rate of 200  $s^{-1}$  after 20 s of preshearing at 10  $s^{-1}$ . The integration time for each data point was 10 s. The gap size was adjusted to 0.2 mm. A mean value was calculated from 8-9 data points.

By a small gap angle  $\theta$  (<5°), the shear rate is approximately constant everywhere within the sample and is given by equation 9:

$$\gamma = \Omega / \theta$$

*Equation 9: Shear rate*

- $\gamma$  ..... Shear rate  
 $\Theta$  ..... Gap angle  
 $\Omega$  ..... Angular velocity of rotating plate

The shear stress on the cone is given by equation 10. C is a constant which depends on the characteristics of the instrument. The data is obtained as shear stress as a function of shear rate and thus eliminating the need of knowing the value of "C" separately.

$$\tau = 3C / 2\pi r^2 \quad \text{Equation 10: Shear stress}$$

- $\tau$  ..... Shear stress  
R ..... Radius of the cone  
C ..... Constant

### 2.2.2.9 Zeta potential

The ZPs of diafiltrated and dialysed LS solutions were measured with a Zetasizer, an instrument that uses Laser Doppler-electrophoresis combined with phase analysis light scattering.

The LS solution was diluted accordingly with ultrapure water. The samples were measured in triplicates in a folded capillary cell with the settings stated in table 9.

**Table 9: Settings of Zetasizer for ZP measurement**

Material: Lignin RI	Dispersant: Water RI	Viscosity [cP]	Scattering angle [°]	Measurement duration automatic
1.355	1.330	0.8872	173	10-50 runs

A 633 nm He-Ne laser was used and the scattered light was detected at an angle of 173°. The ZP can be calculated from the electrophoretic mobility like described in equation 12, which is deduced from the frequency shift of the original and scattered laser (see equation 11).

$$\Delta f = 2v \sin(\theta/2) / \lambda \quad \text{Equation 11: Frequency shift}$$

- f ..... Frequency  
v ..... Particle velocity  
 $\lambda$  ..... Laser wavelength  
 $\theta$  ..... Scattering angle

$$\mu_e = v/E = \epsilon_r \epsilon_0 z / \eta$$

*Equation 12: Helmholtz-Smoluchowski equation*

$\mu_e$  ... Electrophoretic mobility

E ... Electric field strength

$\epsilon_r$  ... Relative permittivity/dielectric constant

$\epsilon_0$  ... Permittivity of vacuum

z ... Zeta potential

$\eta$  ... Viscosity

## 2.2.3 Lignosulfonate polymerization

### 2.2.3.1 Preparation of lignosulfonate solution

For the enzymatic polymerization of lignosulfonates, dried LS powder was dissolved in ultrapure water to obtain the desired 10% and 15% (w/v) solution. The pH was adjusted to 7.0 with sodium hydroxide or sulfuric acid.

### 2.2.3.2 Reaction: Conditions and monitoring

For the polymerization reaction a LS solution was prepared (see chapter 2.2.3.1). The sensor for oxygen monitoring was calibrated like described in chapter 2.2.1.9. The LS solution was transferred in the vessel with the oxygen sensor and placed on the magnetic stirrer (see figure 8).

The LS solution was stirred at 500 rpm and aerated with the help of an immersed airstone, connected to a gas cylinder with pure oxygen, until the LS solution was saturated with oxygen. Afterwards 10 U/mL Mtl was added. From then, oxygen was continuously supplied with 60 cm<sup>3</sup>/min and the oxygen saturation monitored during the whole polymerization process (see chapter 2.2.1.9).

Samples were taken after enzyme addition and then every 30 min during the polymerization process (see chapter 2.2.2.6).

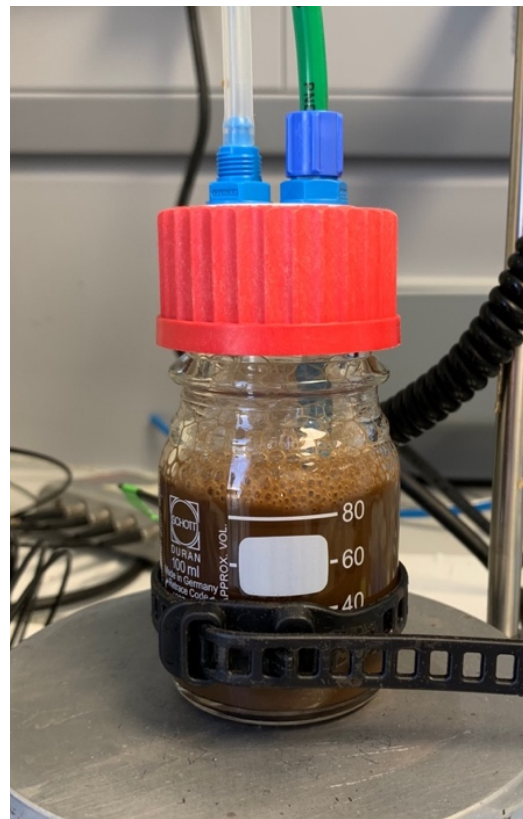


*Figure 8: Polymerization setup*

## 2.2.4 Lignosulfonate treatment

### 2.2.4.1 Thermal treatment of lignosulfonate polymers

LS polymers of 10% and 15% (w/v), were aliquoted and incubated in a water bath at 90 and 100 °C for 40 min. Samples for the determination of enzyme activity, viscosity and MW were taken throughout the heat treatment every 10 min (0-40 min) (see chapters 2.2.1.5, 2.2.2.6 and 2.2.2.8).

The heat treatment was also carried out at 110 °C. Lignosulfonate polymers of 10% and 15% (w/v), were aliquoted and incubated in an autoclave at 110 °C for 20 min. Samples for the determination of enzyme activity, viscosity and MW were taken before and after the heat treatment.

The thermal denaturation kinetics of the laccase were described by the exponential equation 11 and the half life according to equation 12 (Schubert *et al.*, 2015).

$$A_r / A_0 = e^{(-k_d t)}$$

**Equation 13: Denaturation kinetics**

$A_r$  ..... Residual activity after incubation

$A_0$  ..... Initial laccase activity

$k_d$  ..... Rate constant per time

$t$  ..... Duration of incubation

$$t_{1/2} = \ln(2) / k_d$$

**Equation 14: Half-life**

$t_{1/2}$  ..... Laccase half-life

### 2.2.4.2 Storage stability of lignosulfonate polymers

The unpolymerized LS polymers, polymerized LS polymers and the heat treated (90, 100, 110 °C) polymers were aliquoted and stored at 21 °C, either in contact with atmospheric air or saturated with nitrogen. The head space of the bottles used for storage was filled with pure nitrogen before the bottles were hermetically sealed and only opened for sampling. Samples for the determination of enzyme activity, viscosity and MW were taken once per week, over a time range of 35 days (see chapters 2.2.1.5, 2.2.2.6 and 2.2.2.8).

### 3 Results and Discussion

#### 3.1 Characterization of laccase from *Myceliophthora thermophila*

##### 3.1.1 Enzyme purification and size

*Myceliophthora thermophila* laccase was purified by laboratory crossflow ultrafiltration and anion exchange chromatography (see chapter 2.2.1.1 and 2.2.1.2). After chromatography the fractions of purified MtL and MtL that was only purified by ultrafiltration were applied to a SDS gel, which is shown in figure 9 (see also chapter 2.2.1.4.3).

Table 10 shows the position of the samples on the SDS gel and table 11 the respective protein concentration (see chapter 2.2.1.3.2). Ultrafiltrated MtL and fractions A7, A8 and A9 show a strong band around 95 kDa and several smaller bands around 65, 15 and 12 kDa. All other fractions show weak bands around 95 kDa.

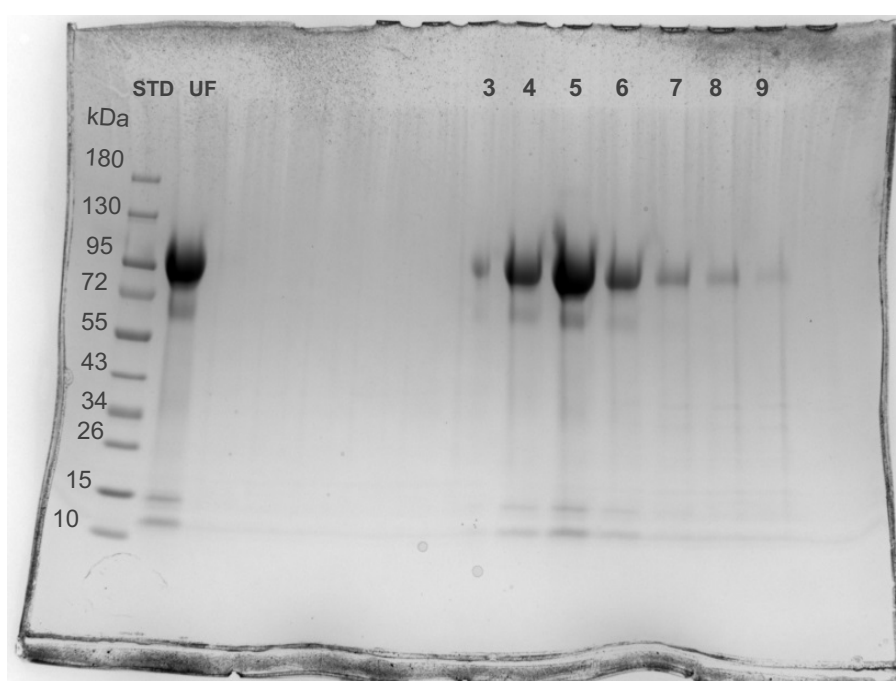


**Figure 9: SDS gel of ultrafiltrated MtL and fractions of purified MtL**

*\*STD...Protein standard, UF...ultrafiltrated enzyme*

**Table 10: SDS gel sample legend and protein concentrations**

Lane	3	4	5	6	7	8	9
Fraction	A6	A7	A8	A9	A10	A11	A12
Concentration [mg/mL]	0.30	0.29	3.83	5.03	1.22	0.65	0.31

It can be assumed that the main band around 95 kDa (see figure 9) is composed of MtL, while the smaller bands represent impurities. The smaller bands, which are also present in fractions A7, A8 and A9, indicate that additional purification with anion exchange chromatography did not result in complete removal of impurities. Fraction 9 had the highest protein concentration (see table 10) and was also used for MW analysis (see chapter 3.1.2).

### 3.1.2 Size and molecular weight of MtL

The MW of MtL was determined in denatured state with electrophoresis and in active state with light scattering. The size of MtL was determined with a DLS instrument and a MALLS detector attached to SEC (see chapter 2.2.1.4).

Figure 10 shows the MW results obtained from the DLS instrument. The mean MW of MtL was determined to be  $65.8 \pm 13.2$  kDa with a size of  $3.6 \pm 0.3$  nm hydrodynamic radius. The big standard deviation (20.1% for MW and 8.3% for size) might be a result of impurities that could have interfered with the measurement.

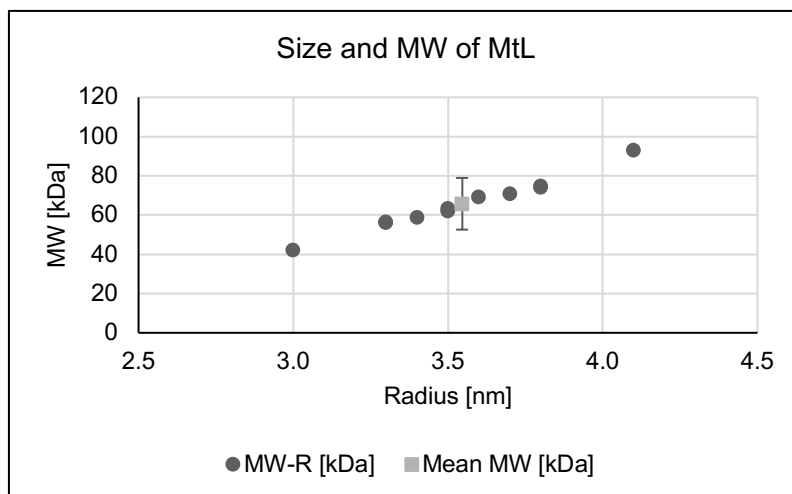


Figure 10: MW and size determination with DLS instrument

Figure 11 shows a chromatogram of purified MtL analyzed by a MALLS detector. The chromatogram shows the distribution curve of MtL and the MW at each slice of the curve. The almost horizontal linear shape of the MW curve through the peak, indicates a monodisperse sample, which could be confirmed by a PDI of 1.01. The MW between a retention

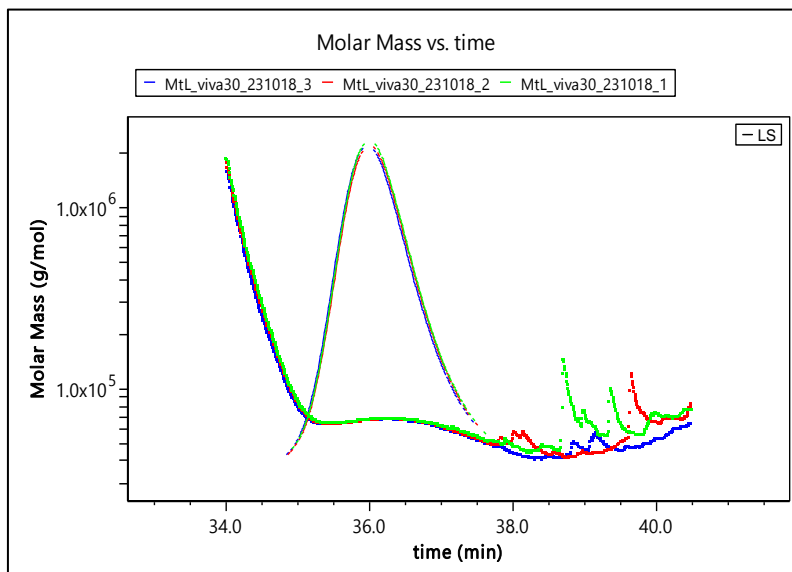


Figure 11: SEC-MALLS chromatogram of purified MtL

time of 35 and 38 min was determined to be  $64.6 \pm 0.5$  kDa, the radius of gyration was  $9.9 \pm 1.4$  nm.

Also a theoretical MW of extracellular laccase lcc1 (see appendix: table 21) was calculated with the ProtParam tool. The MW of MtL was calculated by subtracting the MW of the signal peptide, resulting in 65.5 kDa. This result was only computed from the sequence and did not take into account any post-translational modifications such as glycosylations of the protein.

Table 11 shows a summary of all results of size and MW that were obtained for MtL.

**Table 11: Summary of sizes and MWs for MtL**

	SDS Page	DLS instrument $r_h$	MALLS detector $r_g$	Calculated MW from lcc1 amino acid sequence
Radius [nm]		3.6±0.3	9.9±1.4	
Molecular weight [kDa]	95	65.8±13.2	64.6±0.5	65.5

It is obvious that the size obtained from SDS gel electrophoresis deviates from the sizes obtained by light scattering and calculated MW. Regarding this, it has to be mentioned that MtL is denatured for gel electrophoresis and therefore measured in a defolded state. This might cause a steric effect that leads to overestimation of the MW. Also covalently attached carbohydrates contribute to this effect (López-Cruz, Viniegra-González and Hernández-Arana, 2006). For both light scattering methods the resulting MWs were in a similar range. However, it has to be stated that MALLS detection is based on 18 angles for light scattering and additionally the concentration is detected by RI, which gives more accurate results than instruments where only 1 scattering angle is used (DLS instrument). Therefore the MW of 64.6±0.5 nm obtained from MALLS was used for further calculations (see chapter 3.1.2). The MW based on the amino acid sequence of extracellular laccase lcc1 is 65.5 kDa but did not take glycosylation into account. Usually the radius of gyration is estimated smaller than the hydrodynamic radius (see chapter 1.1.4.5), which is not represented in this data. However, as explained above, the result of 9.9±1.4 nm radius of gyration obtained from MALLS detection is probably more accurate and reliable.

### 3.1.3 Enzymatic kinetics of MtL

To determine the catalytic constants of purified MtL, activities at different substrate concentrations were determined (see chapter 2.2.1.7). For the calculation of the constants the protein concentration was determined as described in chapter 2.2.1.3.1 (see table 12).

Figure 12 shows the Michaelis-Menten plot of MtL; the reaction velocity increases with increasing substrate concentrations until  $v_{max}$  is reached at 1548.3 U/mL. For the calculation of the catalytic constants of purified MtL the protein concentration was determined with a Bradford protein assay, resulting in 8.7±0.1 g/L. Table 12 shows the calculated catalytic constants of purified MtL.

**Table 12: Catalytic constants of purified MtL**

$v_{max}$ [mM min <sup>-1</sup> ]	$v_{max}$ [M s <sup>-1</sup> ]	$K_M$ [μM]	Conc. [g/L]	MW [g/mol]	E [M]	$k_{cat}$ [s <sup>-1</sup> ]	$k_{cat}/K_M$ [s <sup>-1</sup> M <sup>-1</sup> ]
1548.3	2.6 x 10 <sup>-2</sup>	832.4	8.7±0.1	64600	1.3 x 10 <sup>-4</sup>	192.4	2.3 x 10 <sup>5</sup>

The obtained catalytic constants differ significantly with constants found in literature (see table 13).

**Table 13: Catalytic constants from Mtl with ABTS as substrate compared to values from literature**

Source	$K_M$ [ $\mu\text{M}$ ]	$k_{\text{cat}}$ [ $\text{s}^{-1}$ ]	$k_{\text{cat}}/K_M$ [ $\text{s}^{-1} \text{M}^{-1}$ ]	Conditions
Novozym 51003 (own results)	832.4	192.4	$2.3 \times 10^5$	23 °C, 50 mM NaPi pH 7.0
Novozym DeniLite IIs (López-Cruz et al. 2006)	49.5	601	$6.9 \times 10^7$	25 °C, 50 mM NaPi pH 6.0

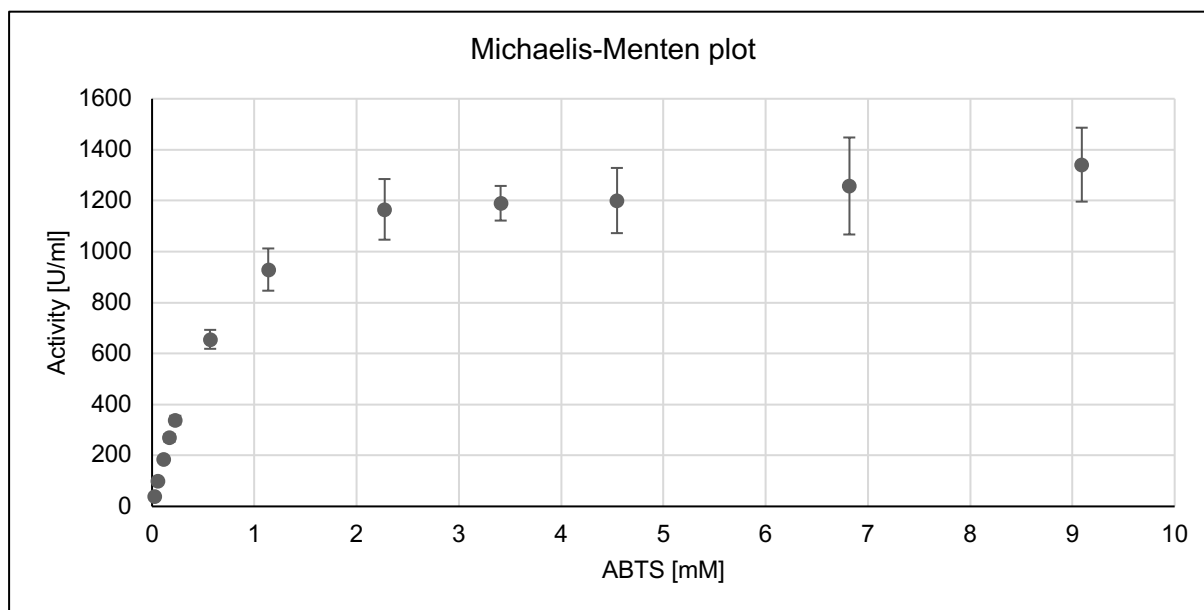


**Figure 12: Michaelis-Menten plot of purified Mtl with ABTS as substrate**

The  $K_M$ -value was determined to be 832.4  $\mu\text{M}$ . This results differ from the result 49.5  $\mu\text{M}$  stated by López-Cruz (López-Cruz, Viniestra-González and Hernández-Arana, 2006), which means that under the given conditions the affinity of our enzyme to the substrate is lower in comparison to the enzyme that was used in these previous studies.

A turnover number ( $k_{\text{cat}}$ ) of 192.4  $\text{s}^{-1}$  means that less substrate molecules are converted into product in comparison to the  $k_{\text{cat}}$  from literature, where 601 substrate molecules are turned over per second. The turnover numbers of most enzymes with their physiological substrates are in the range of 1 to 10 000  $\text{s}^{-1}$  (Berg, Tymoczko and Stryer, 2013).

The differences in obtained constants could be due to the usage of a different buffer and due to the varying temperature at which the activity was determined, since the  $K_M$  value for an enzyme depends on the particular substrate and on environmental conditions such as pH, temperature, and ionic strength (Berg, Tymoczko and Stryer, 2013). Of course, there is also the possibility that these two enzymes, stated to be *Myceliophthora thermophila* laccase, differ in their sequences and might differ in their enzymatic properties.

### 3.1.4 Storage stability of MtL

To determine the best storage conditions for purified and unpurified MtL, aliquots of diluted and undiluted enzyme were stored at different temperatures (see chapter 2.2.1.8).

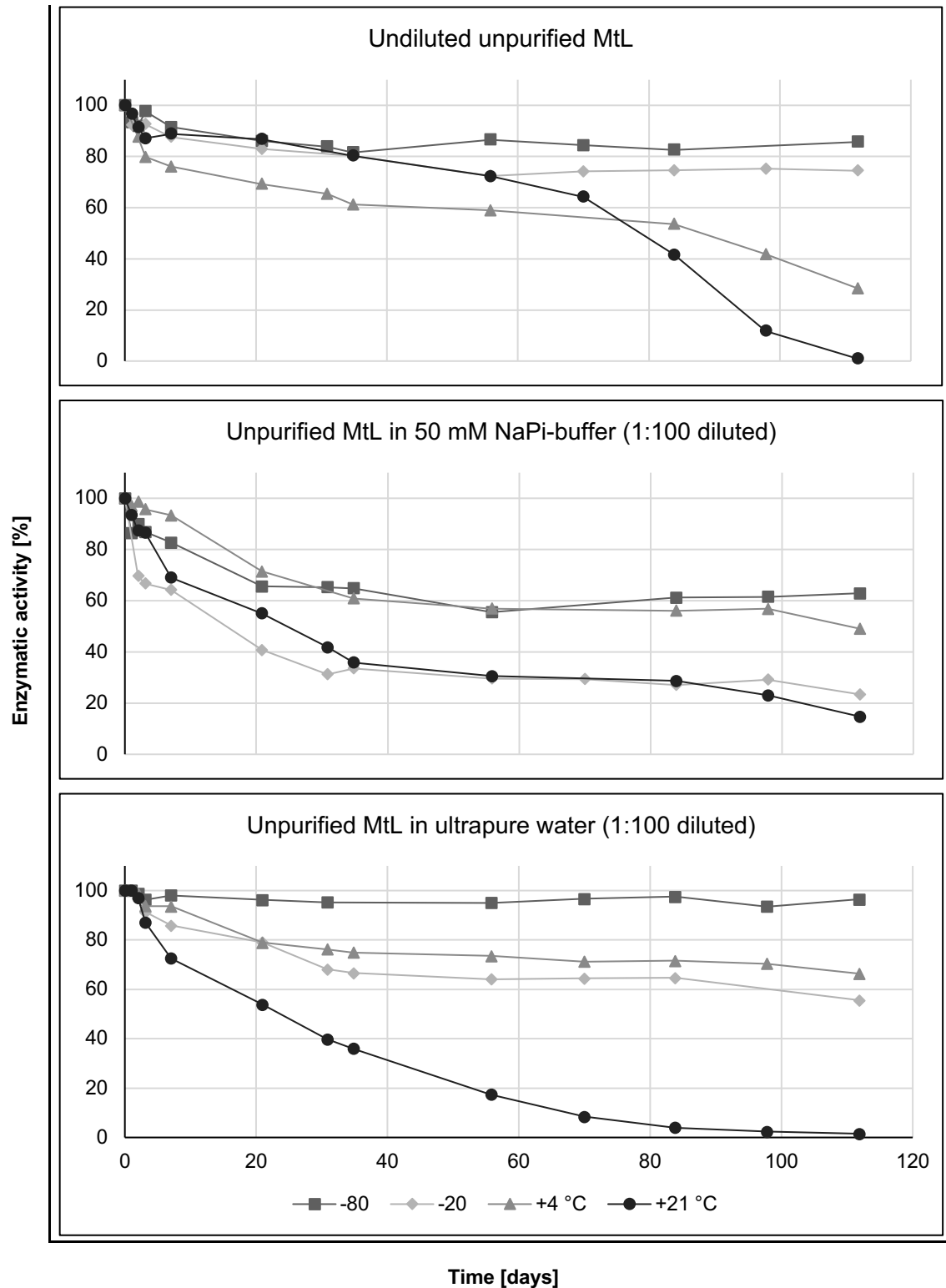


Figure 13: Storage stability of unpurified MtL at different temperatures

Figure 13 shows the course of activity of unpurified MtL over a time period of 112 days. The undiluted and unpurified enzyme solution equals the original Novozym 51003 solution. After 112 days of storage undiluted unpurified MtL showed a decrease in activity to 75% if stored at -20 °C and a decrease to 85% if stored at -80 °C. In contrast to that, at a storage temperature of +4 °C the activity decreased to 28%, while the enzyme stored at +21 °C showed no residual activity after 112 days. Unpurified MtL that was diluted 1:100 in 50 mM NaPi-buffer surprisingly showed similar results for -20 °C and +21 °C storage temperature. At these temperatures a residual activity of 15-23% was measured. Also the results for storage temperatures of +4 and -80 °C were similar. After 56 days the activity decreased to 56-57%, while after 112 days the residual activity was only 49-63%.

The biggest activity difference for different storage temperatures was observed for unpurified MtL that was diluted 1:100 in ultrapure water. The highest residual activity was observed for a storage temperature of -80 °C. The residual activity at this temperature was 95% after 112 days. An exponential decrease in activity to only 2% was observed at a storage temperature of +21 °C. The results for storage temperatures of -20 °C and +4 °C were similar with a decline of activity to 56-66%.

In general it can be noticed that freezing at -80 °C is the best way to preserve enzymatic activity during storage, while storage at +21 °C would lead to an activity loss of at least 85% within 4 months. Surprisingly the storage in ultrapure water is more beneficial compared to buffer when the enzyme solution is frozen/cooled. Only at +21 °C the decline in activity is faster when the enzyme is diluted in ultrapure water.

Figure 14 shows the results of enzymatic activity during storage of purified MtL. The first graph shows the change in activity of undiluted purified MtL over 98 days. The storage at +21 °C showed almost a linear decay down to 9% residual activity. In contrast, MtL stored at +4, -20 or -80 °C showed an activity of 84-89% after 98 days. The most surprising results were obtained during the storage of purified MtL diluted 1:100 in buffer. During the storage at -20 °C a 70% decrease in activity was observed after the first day of storage. Afterwards the activity remained constant at 30% during the whole storage experiment. Also surprisingly was the activity decay during the storage at -80 °C. In all other cases when MtL was stored at -80 °C, the activity had the highest value in comparison to all other storage temperatures, which was not the case here. Purified MtL 1:100 diluted in buffer, which was stored at +4 °C showed the highest activity. The activity at +4 °C storage temperature was also constant. A more or less linear activity decrease was observed at a storage temperature of +21 °C.

The purified MtL that was diluted 1:100 in ultrapure water showed also a more or less linear decrease in activity if stored at +21 °C. Like in the case of MtL that was diluted 1:100 in buffer,

with the difference that the observed slope curve is not so steep. The activity at storage temperatures +4, -20 and -80 °C could be considered as constant.

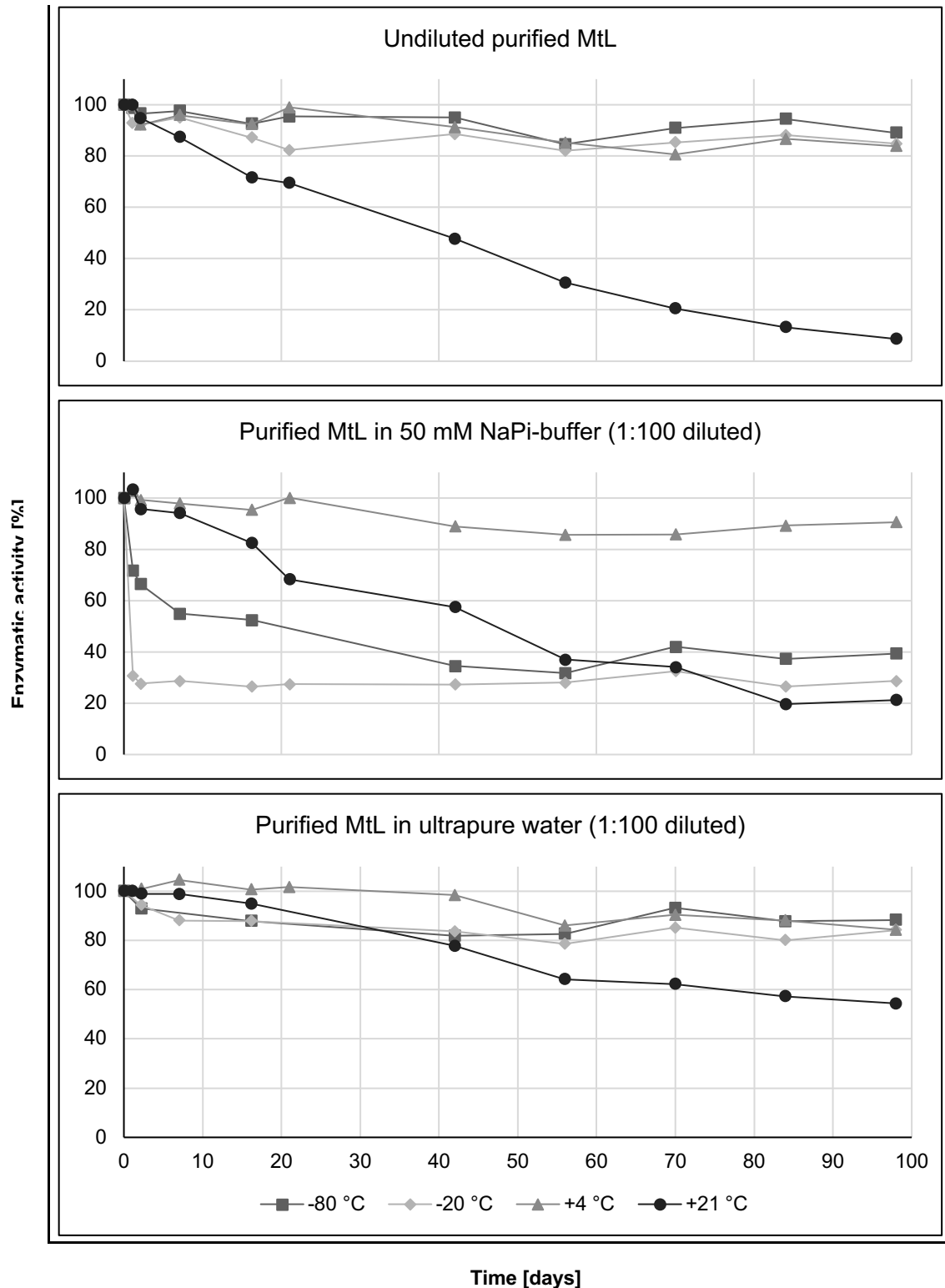


Figure 14: Storage stability of purified MtL at different temperatures

### 3.1.5 Influence of temperatures on MtL activity

#### 3.1.5.1 Activity maximum with varying temperature

To determine the activity maximum of MtL, the activity determination was carried out at different temperatures as described in chapter 2.2.1.6.

Figure 15 shows that the activity of unpurified and purified MtL at different temperatures between 35 and 70 °C. For unpurified MtL an activity maximum was determined at 60 °C, while for purified MtL the highest activity was observed at 65 °C, which led to the assumption that the activity maximum would be between 60 and 65 °C. These results could be confirmed by similar results from commercial MtL found in literature. In these studies MtL was stated to show denaturation

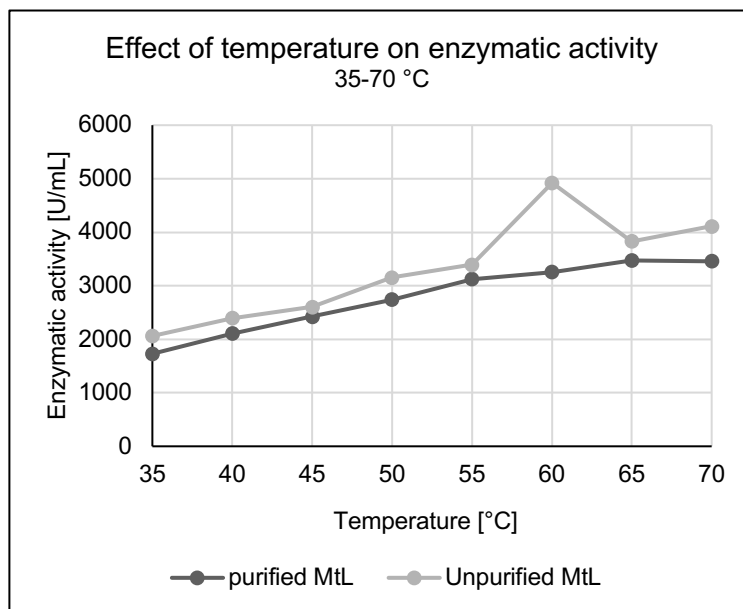


**Figure 15: Activity of unpurified and purified MtL at temperatures from 35 to 70 °C**

effects at temperatures higher than 70 °C, while the activity maximum was around 65 °C. (López-Cruz, Viniegra-González and Hernández-Arana, 2006) Unfortunately, it was not possible to measure the activity above 70 °C due to technical limitations.

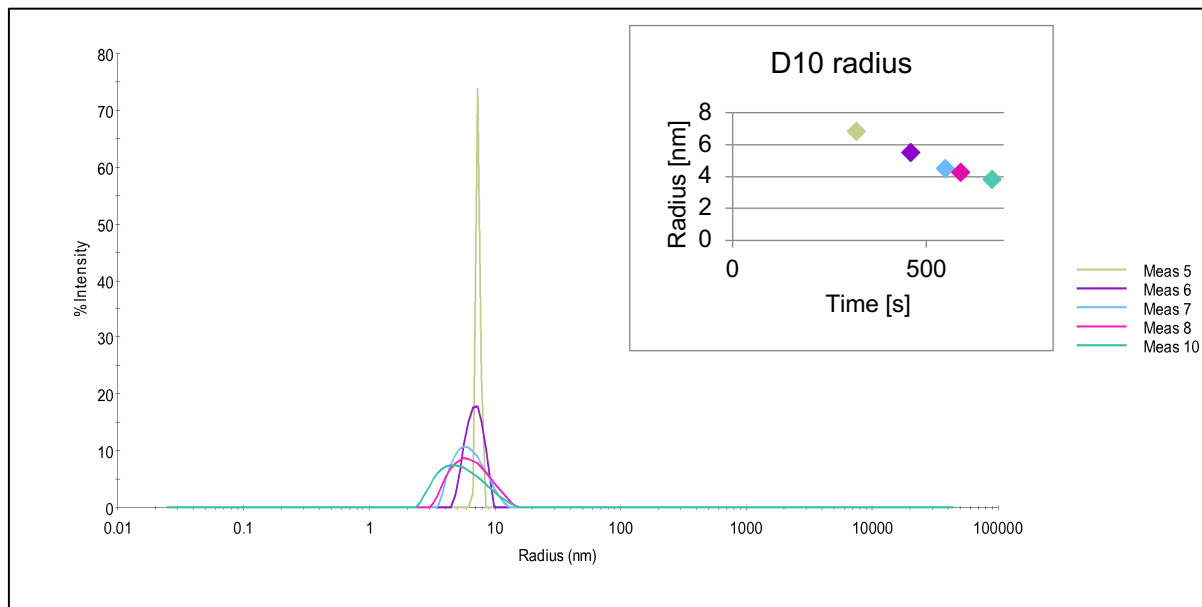
#### 3.1.5.2 Effect of high temperatures

To determine the denaturation temperature of MtL, the  $R_h$  was measured after a heat treatment of the enzyme as described in chapter 2.2.1.4.1 and 3.1.2.

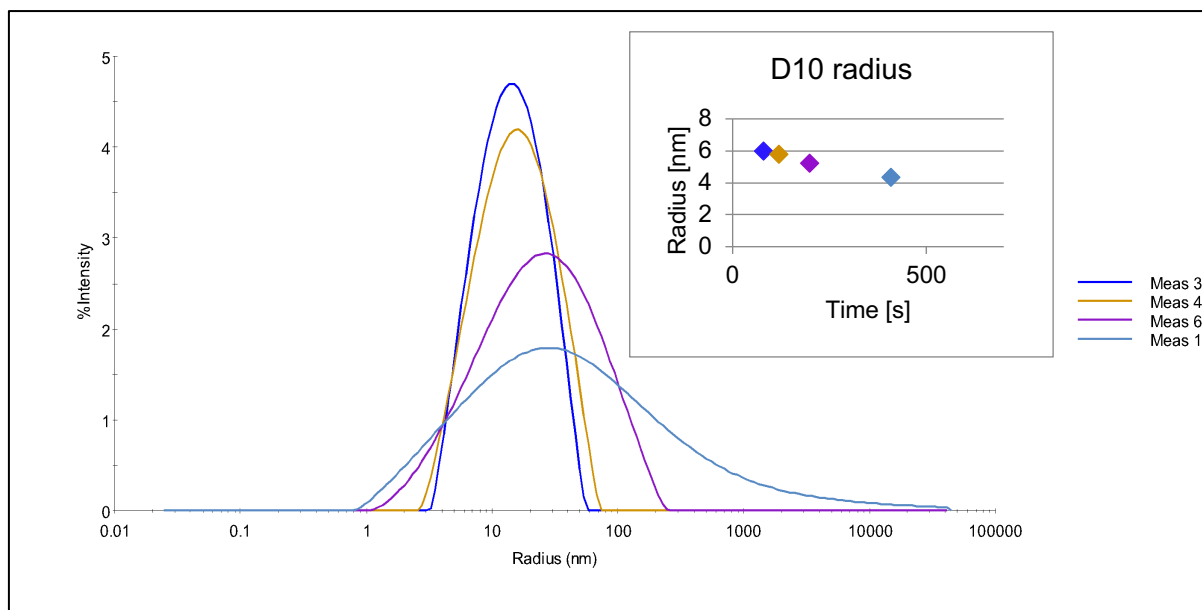
Figure 16 shows the change of size distributions of  $R_h$  over time after a heat treatment at 90 °C. Measurements 5, 6, 7, 8 and 10 were selected for data analysis. It can be observed that the  $R_h$  distributions tend to shift to smaller radii over time. Also the D10 radii show a decrease over time. These observations might indicate that the laccase is refolding again after a treatment at 90 °C, which might result in a refolded and native form of the enzyme.

Figure 17 shows the change of size distributions of  $R_h$  over time after a heat treatment at 95 °C. Measurements 3, 4, 6 and 11 were selected for data analysis. The  $R_h$  distributions changed over time. The peaks broadened and thereby shifted to smaller but also bigger radii. While

bigger radii indicate a denaturation of the enzyme, smaller radii might indicate a refolding of the enzyme.



**Figure 16: Size distributions of hydrodynamic radii over time after 90 °C heat treatment**



**Figure 17: Size distributions of hydrodynamic radii over time after 95 °C heat treatment**

Figure 18 shows the change of size distributions of  $R_h$  over time after a heat treatment at 99 °C. For data analysis measurements 1, 6 and 10 were selected. Figure 18 reveals similar results as already observed in figure 17.

These findings indicate that laccase could not be denatured irreversibly under these conditions (10 min, 95-99 °C). Complementing to these results, activity assays were performed after treatments at different temperatures (see chapter 3.2.3).

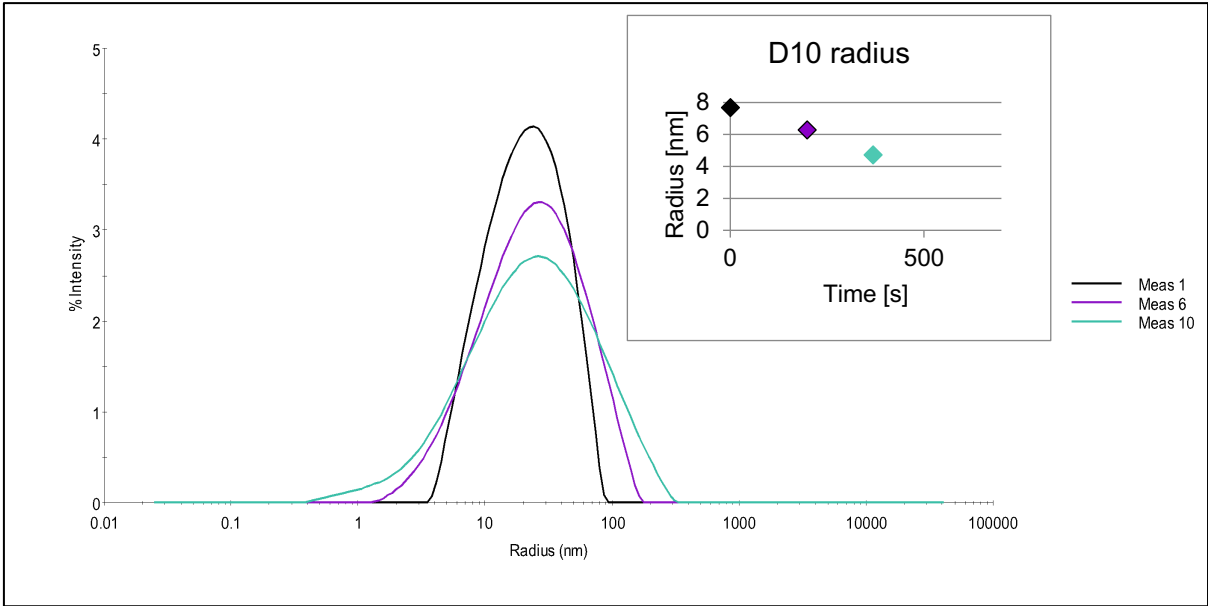


Figure 18: Size distributions of hydrodynamic radii over time after 99 °C heat treatment

## 3.2 Lignosulfonate polymerizations

### 3.2.1 Properties of raw material

To determine different properties of the raw material different analyses were carried out as described in chapters 2.2.2.3 - 2.2.2.6, 2.2.2.8 and 2.2.2.9.

The properties of the raw material are shown in tables 14 and 15.

**Table 14: Properties of the raw material**

Lignosulfonate (w/v)	pH	MW [kDa]	PDI $M_w/M_n$	Viscosity [mPas]	Phenol content [mmol/L]	ZP [mV]	Conductivity [mS/cm]
10%	4.0	180.5±7.8	1.64±0.10	4.6±0.0	110.2±1.5	-20.27±1.18	0.28±0.01
15%				8.3±0.0	173.0±0.2		

Table 14 shows the properties of the LS solution used in this work. The LS solution had a pH of 4. The 10% (w/v) solution showed a viscosity of 4.6±0.0 mPas and the 15% (w/v) solution 8.3±0.0 mPas. The mean MW of the 10% and 15% (w/v) solution resulted in a size of 180.5±7.8 kDa whereby the mean PDI was 1.64±0.10. A phenol content of 110.2±1.5 mmol/L was determined for the LS solution with 10% (w/v) and a higher phenol content of 173.0±0.2 mmol/L for the 15% (w/v) solution. After dialysis the 10% (w/v) LS showed a zeta potential of -20.27±1.18 mV and a conductivity of 0.28±0.01 mS/cm.

**Table 15: The S/G ratio of the raw material**

Raw material	S (1327 $\text{cm}^{-1}$ )	G (1262 $\text{cm}^{-1}$ )	S/G
FTIR	0.02	0.11	0.18

Table 15 shows the S/G ratio of the raw material. For S/G ratio estimation the intensities of the bands around 1320  $\text{cm}^{-1}$  (S-units) and 1268  $\text{cm}^{-1}$  (G-units) were estimated ('Evaluating Lignin-Rich Residues from Biochemical Ethanol Production of Wheat Straw and Olive Tree Pruning by FTIR and 2D-NMR', 2015). An intensity of 0.02 for the S-unit and 0.11 for the G-unit was obtained, resulting in a S/G ratio of 0.18. The significantly higher G-units content in our lignin, means that the used lignin is a softwood lignin, since according to literature, softwood lignin is mainly built up from G-units (up to 95%) (Christopher, Yao and Ji, 2014).

### 3.2.2 Monitoring of polymerizations

To monitor the changes of LS during polymerization, different analyses were carried out as described in chapters 2.2.1.9, 2.2.2.3, 2.2.2.4 and 2.2.2.6.

Figure 19 shows the oxygen curve during polymerization of 10% and 15% (w/v) LS solutions. After the LS solution was completely saturated with pure oxygen, laccase was added, which resulted in an immediate decline of dissolved oxygen. This effect is typically observed from laccase, which reduces oxygen to water. It can be assumed that dissolved oxygen was immediately consumed by laccase, which results in an oxygen saturation of 0% throughout the reaction.

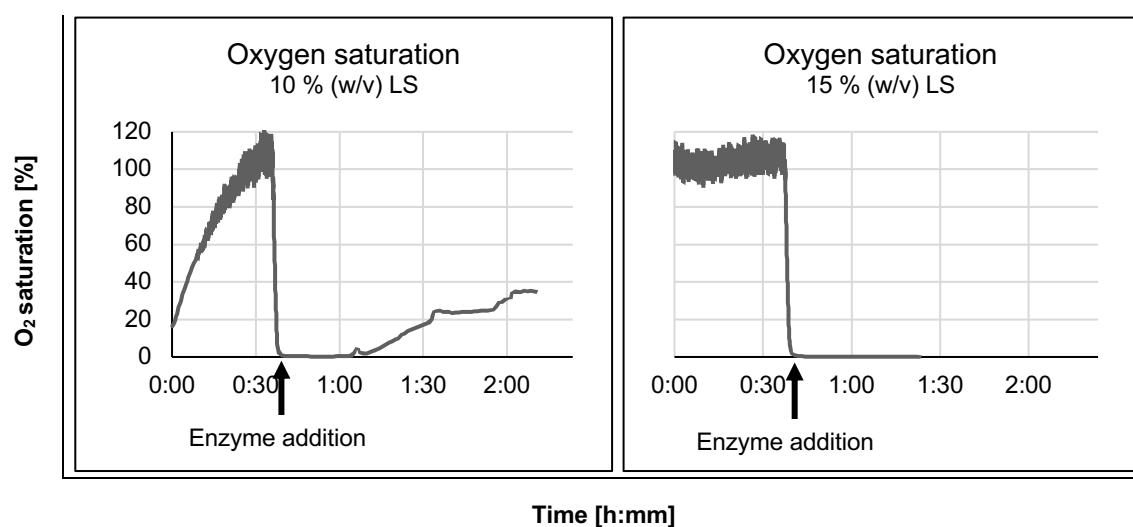


Figure 19: Oxygen saturation during polymerization

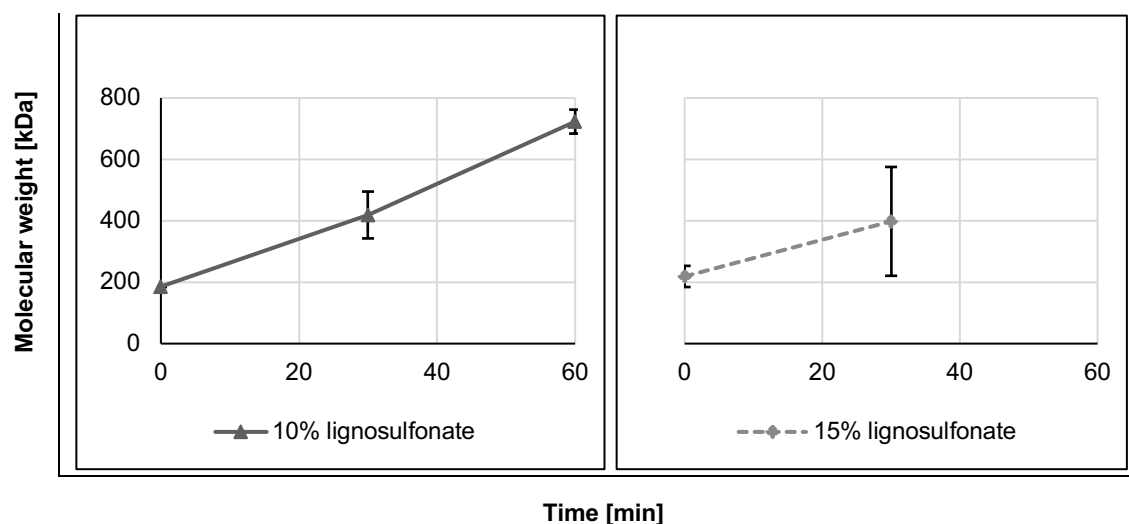
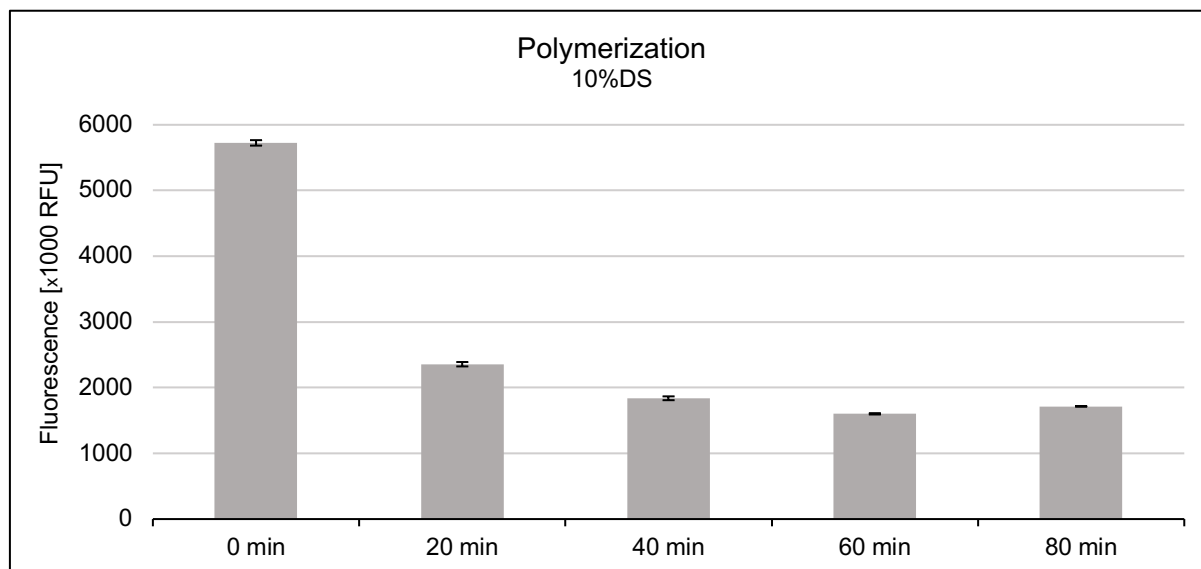


Figure 20: Increase of molecular weight during polymerization

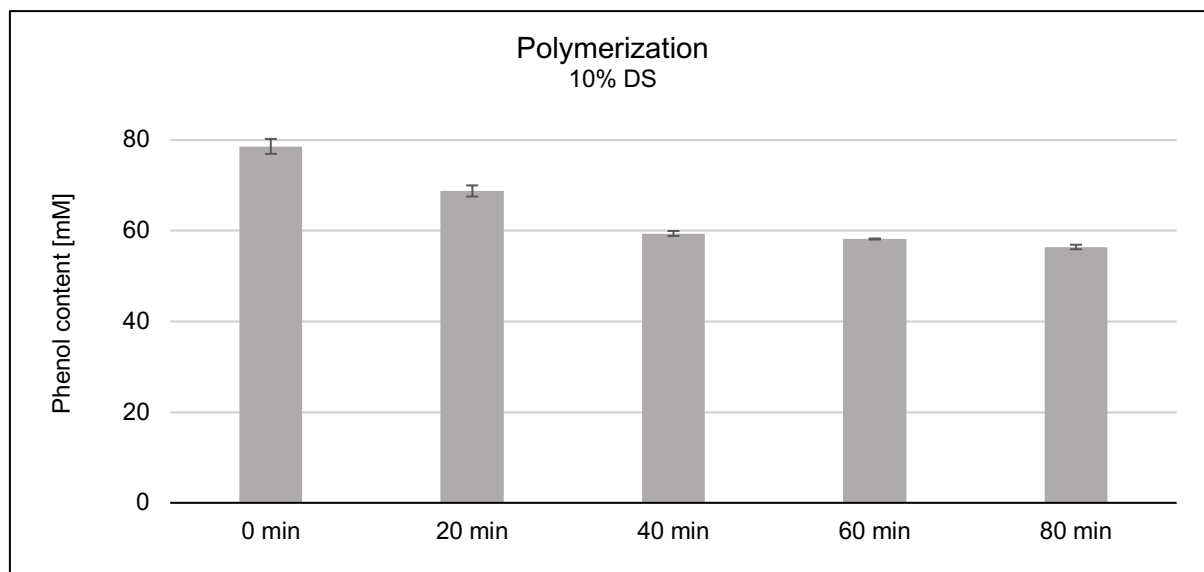
Figure 20 shows the increase of MW during the polymerization process. The raw material had a mean MW of  $180.5 \pm 7.8$  kDa. For 15% (w/v) LS polymers, the MW was  $398.2 \pm 177.3$  kDa

after 30 min, while for 10% (w/v) polymers a MW of  $723.1 \pm 39.0$  kDa could be obtained after 60 min. While in previous studies, polymerizations with highest possible MWs were the main goal, in these studies we focused more on mechanistic aspects to make the process controllable and gain a defined and stable product in the end. For that reason, polymerizations were stopped after 45 min (15% LS) and 90 min (10% LS) to avoid polymers to get insoluble due to extensive polymerization.

Figure 21 shows the decline in fluorescence during the polymerization reaction. The fluorescence drops from 5700000 RFU to 2360000 RFU within the first 20 min of polymerization. Afterwards the fluorescence further decreases to 1600000-1700000 RFU until the end of the polymerization process. A decrease in fluorescence indicates that laccase catalyzed polymerization causes a modification of fluorescing lignin molecules. The polymerization reaction was linked in previous studies already to a decrease in fluorescent units. (Ortner et al 2015; Huber et al 2016)



**Figure 21: Fluorescence during polymerization**



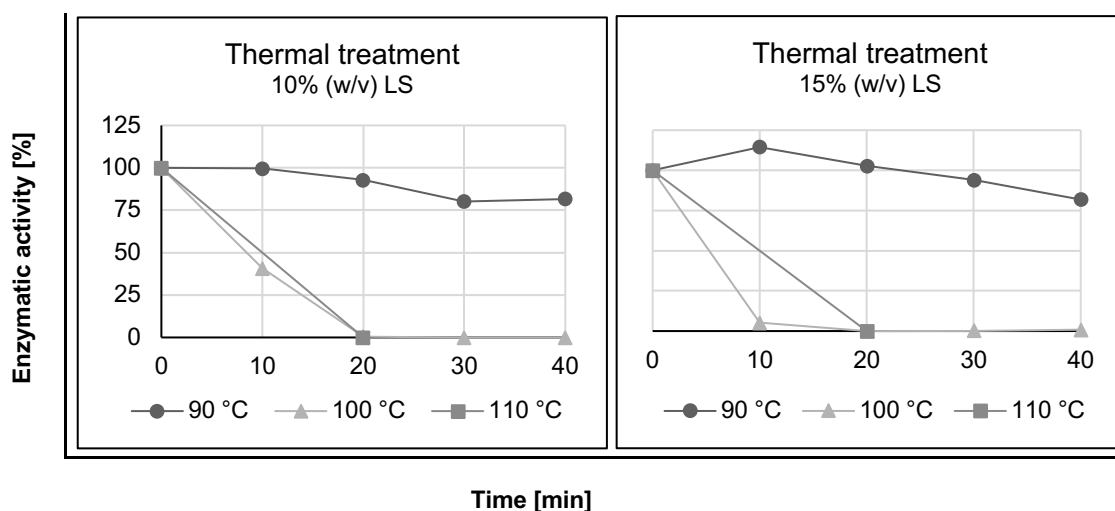
**Figure 22: Phenol content during polymerization**

Figure 22 shows the decline of the phenol content during the polymerization reaction of LS polymers. The phenol content was  $78.6 \pm 1.7$  mmol/L at the start of the reaction and decreased to  $56.4 \pm 0.3$  mmol/L within 80 min of laccase catalyzed polymerization. During the oxidation process of LS, phenoxy radicals are created and react with each other and surrounding molecules, which changes the content of phenolic groups. Monitoring of changes in phenolic groups thereby provides information on the extent of polymerization. (Ortner et al 2015)

Summarizing, it can be said that LS polymers could be successfully polymerized during this reaction, which could be demonstrated by an increase in MW and a decrease in oxygen saturation, fluorescence and phenolic content.

### 3.2.3 Influence of different temperatures on polymers and enzymatic activity

To analyze the influence of different temperatures on the LS polymers and the enzymatic activity, experiments at different temperatures were carried out as described in chapter 2.2.4. Additionally the thermal stability coefficients were calculated (see chapter 2.2.4.2).



**Figure 23: Enzymatic activity during thermal treatments at 90, 100 and 110 °C.**

Figure 23 shows the change of enzymatic activity during thermal treatments at 90, 100 and 110 °C. A thermal treatment at 90 °C for 40 min caused a decrease of enzymatic activity to 82% for both lignin concentrations, which shows basically no denaturation effect of the enzyme. Also according to literature, enzymatic activity of MtL was increasing in a range from 40-90 °C (Ibarra *et al.*, 2006). In contrast to that, incubation of the samples at 110 °C for 20 min caused a complete inactivation of the enzyme with no residual activity. For 10% LS samples an incubation at 100 °C showed a decline of enzymatic activity to only 0.5% residual activity within 20 min, while for 15% LS samples the enzymatic activity decreased to 5.1% within 10 min and no residual activity could be measured after 20 min incubation time.

**Table 16: Thermal stability coefficients of MtL in lignosulfonate solution**

Temperature [°C]	10% (w/v) lignosulfonate		15% (w/v) lignosulfonate	
	$k_d$ [h <sup>-1</sup> ]	$t_{0.5}$ [h]	$k_d$ [h <sup>-1</sup> ]	$t_{0.5}$ [h]
100	15.85	0.044	17.82	0.039
110	n.a.	n.a.	n.a.	n.a.

Table 16 shows the thermal deactivation constant ( $k_d$ ) and the half-life ( $t_{0.5}$ ) of MtL in 10 or 15 % (w/v) LS solution during thermal treatments. As expected,  $k_d$  increases with increasing temperatures. Lower  $k_d$  values are an indicator that the enzyme is more stable at the given conditions (Schubert *et al.*, 2015). Regardless of the obtained results of this experiment, MtL was stated earlier to follow an exponential decay model, which could not be shown here due to a lack of sampling during the experiment (Gouveia *et al.*, 2012). For the 100 °C incubation, MtL in the 15% lignin sample had a higher thermal deactivation constant indicating the enzyme to be less thermostable in solutions with higher lignin content. The enzymes half-life was between 0.039 and 0.044 h for incubation at 100 °C. This result was comparable to earlier

studies, stating a half-life of 0.05 h for MtL according to activity studies at different temperatures (Ibarra *et al.*, 2006).

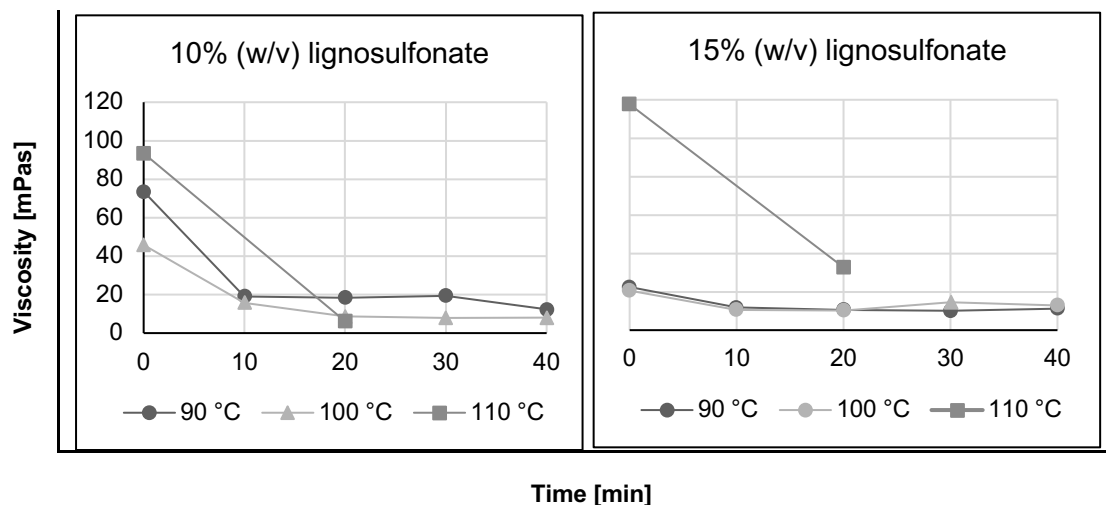


**Figure 24: Viscosity decline during thermal treatment.**

The samples drawn during the incubation at different temperatures were also analyzed regarding viscosity. Figure 24 shows the viscosity of 10% and 15 % (w/v) LS solutions. For 10% lignin concentration, the viscosity decreases from 46-93 mPas to 6-20 mPas within 20 min and stays almost constant during the remaining incubation time. For 15% lignin concentration a big difference could be observed between experiments at 90 and 100 °C compared to 110 °C. For 110 °C a decrease from 118 to 33 mPas was measured. Lignosulfonate polymers (15%) that were incubated at 100 and 90 °C showed a decrease from 22 to 10-13 mPas.

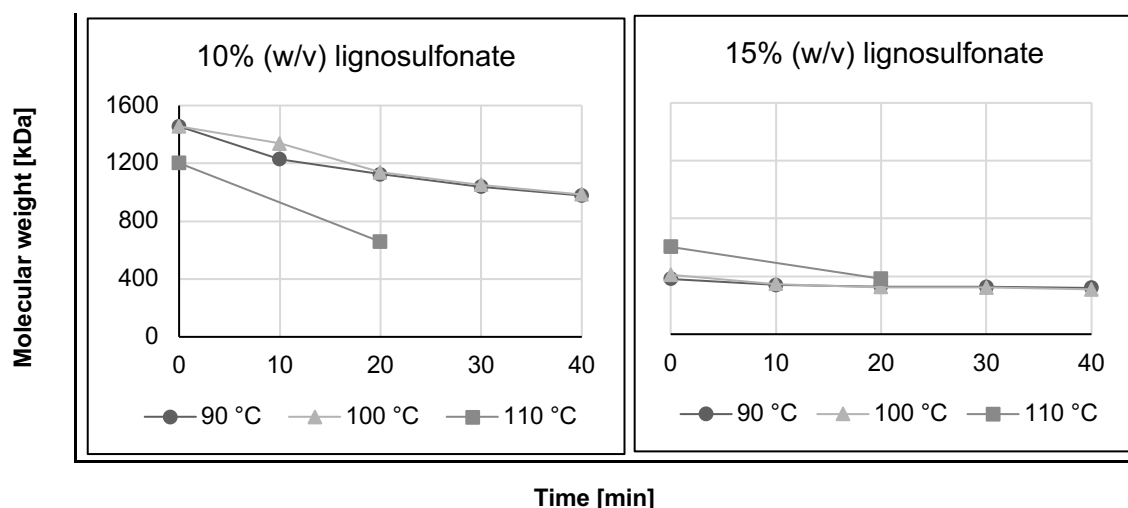


**Figure 25: Molecular weight decline during thermal treatment.**

Figure 25 shows the MWs of LS polymers during incubation at different temperatures. In total the MW of 10% (w/v) LS polymers decreased from 1460 to 980 kDa at 90 and 100 °C, while

at 110 °C the MW decreased from 1200 to 660 kDa. The MW of 15% LS solution treated at 90 and 100 °C decreased from 380-410 to 310-320 kDa within 40 min incubation time. 15% (w/v) LS solution treated for 20 min at 110 °C showed a decrease of MW from 600 to 380 kDa. However, as explained above (see figure 23) the enzyme could only be deactivated at 100 and 110 °C. From the results at 100 °C the MWs of 15% (w/v) LS solution decrease to a lower extent of 24% compared to 10% (w/v) solution, where a decrease of about 32% takes place during incubation.

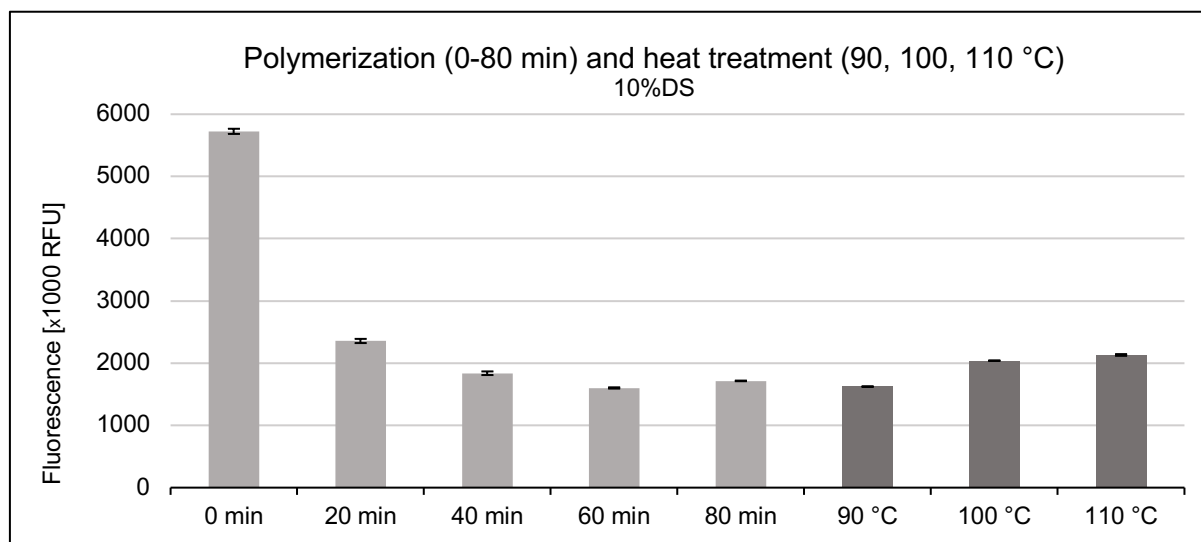


**Figure 26: Fluorescence during polymerization and after thermal treatment.**

As explained above (see figure 21) fluorescence decreases during polymerizations. Figure 26 shows additionally the fluorescence of LS samples after thermal treatment. It can be observed that fluorescence increases again after a heat treatment at 100 and to a even higher extent at 110 °C. This might indicate a reversed effect, namely the breakage of lignin bonds. However, this effect could not be observed for incubation at 90 °C.

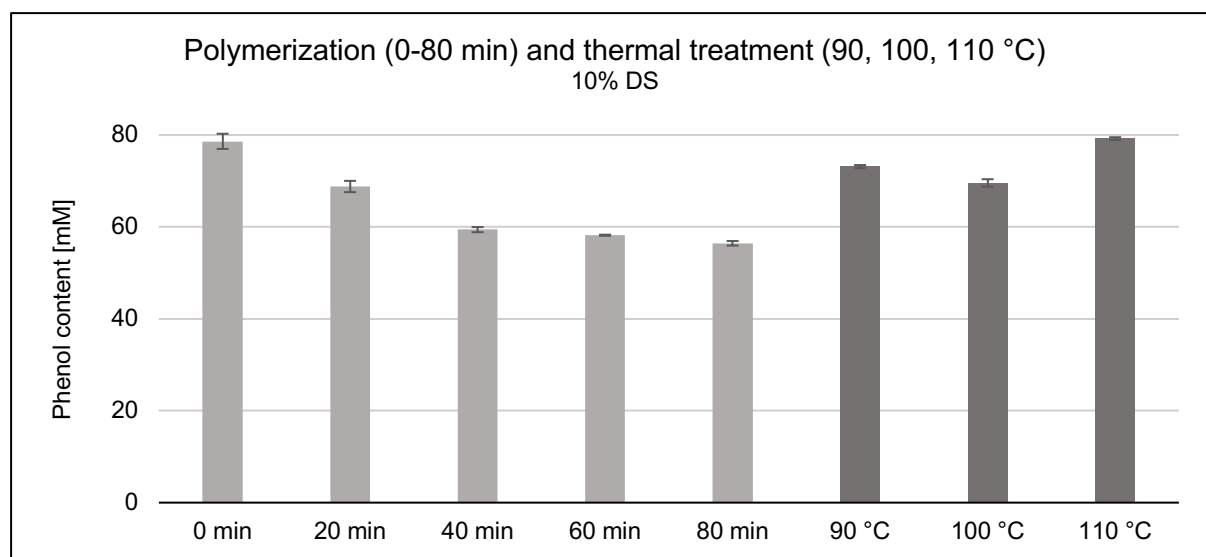


**Figure 27: Phenol content during polymerization and after thermal treatment.**

Figure 27 shows the phenol content during polymerization (see also figure 22) and additionally the phenol contents of LS samples after heat treatment at 90, 100 and 110 °C. For samples incubated at 90, 100 and 110 °C it can be observed that the content of phenolic hydroxyl groups increased again after polymerization from  $56.4 \pm 0.3$  mmol/L (80 min) to  $69.6 \pm 0.3$  -  $79.2 \pm 0.8$  mmol/L. This might indicate that the phenol content either increases by formation of new phenolic hydroxyl groups or by bond breakage caused through thermal treatment.

### 3.2.4 Storage stability of lignosulfonate polymers

To determine the storage stability of LS polymers, samples were stored in air or nitrogen and monitored by enzymatic activity, viscosity and MW.

Figure 28 shows the enzymatic activity of MtL measured during a storage period of up to 35 days. It can be observed that no significant difference in enzyme activity is noticeable between samples stored in contact with air or nitrogen. Furthermore, it can be noticed that the enzymatic activity in samples treated at 90 °C is even higher than in the reference (untreated sample). Together with the findings in chapter 3.1.5.2 it can be assumed that the laccase could not be deactivated and is therefore active after a heat treatment at 90 °C.

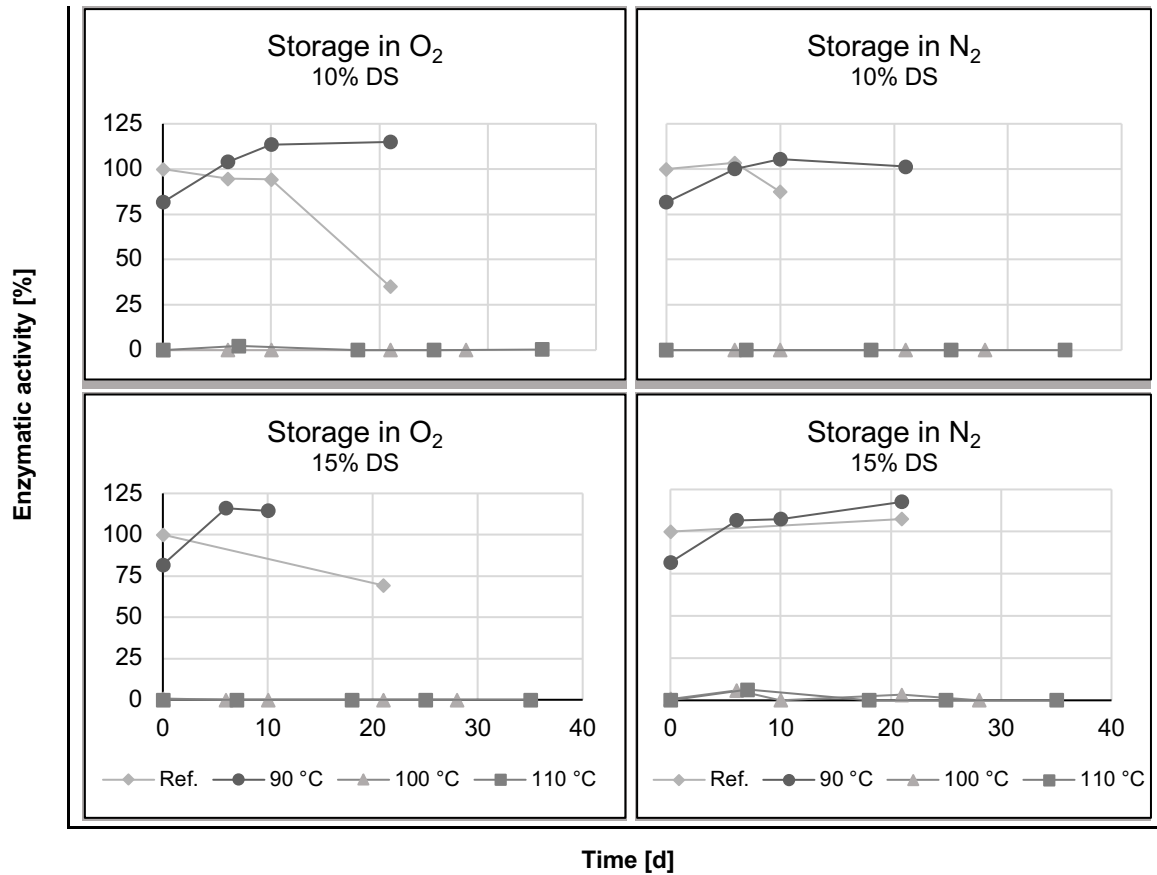


Figure 28: Enzymatic activity during different storing conditions

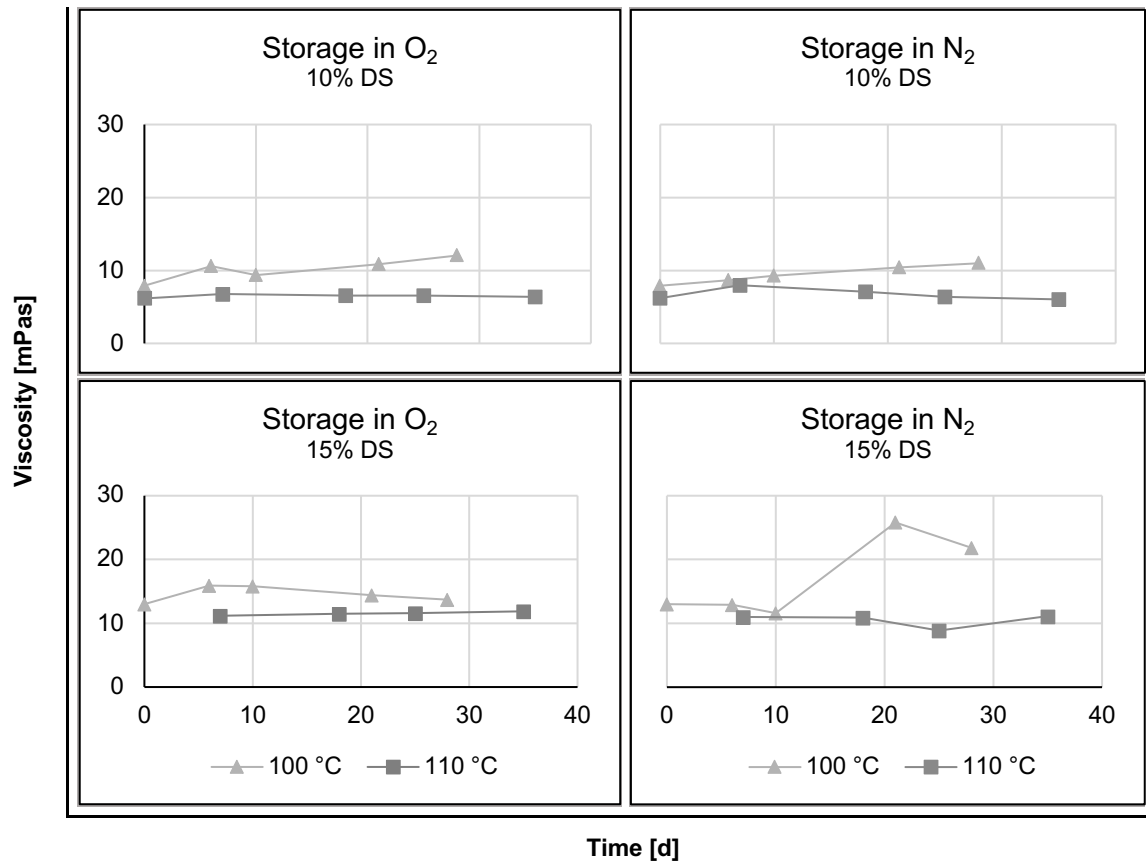


Figure 29: Viscosity of LS samples stored at different conditions

After treating the enzyme at 100 °C for 40 min or 110 °C for 20 min no activity could be observed during the storage period of 35 days, which indicates a complete deactivation.

Figure 29 shows the viscosity of LS solutions during a storage period of 35 days. It can be observed that the viscosity for 10% (w/v) LS solution after incubation at 110 °C was constantly between 6 and 8 mPas, while after incubation at 100 °C the variation was slightly bigger within 8 and 12 mPas. For 15% (w/v) LS solution the heat treatment at 110 °C resulted in a variation between 9 and 12 mPas, while the viscosity of samples treated at 100 °C showed values between 12 and 26 mPas.

Viscosity measured for samples treated at 90 °C and reference samples (untreated) did not produce reliable results due to polymerization and aggregation effects.

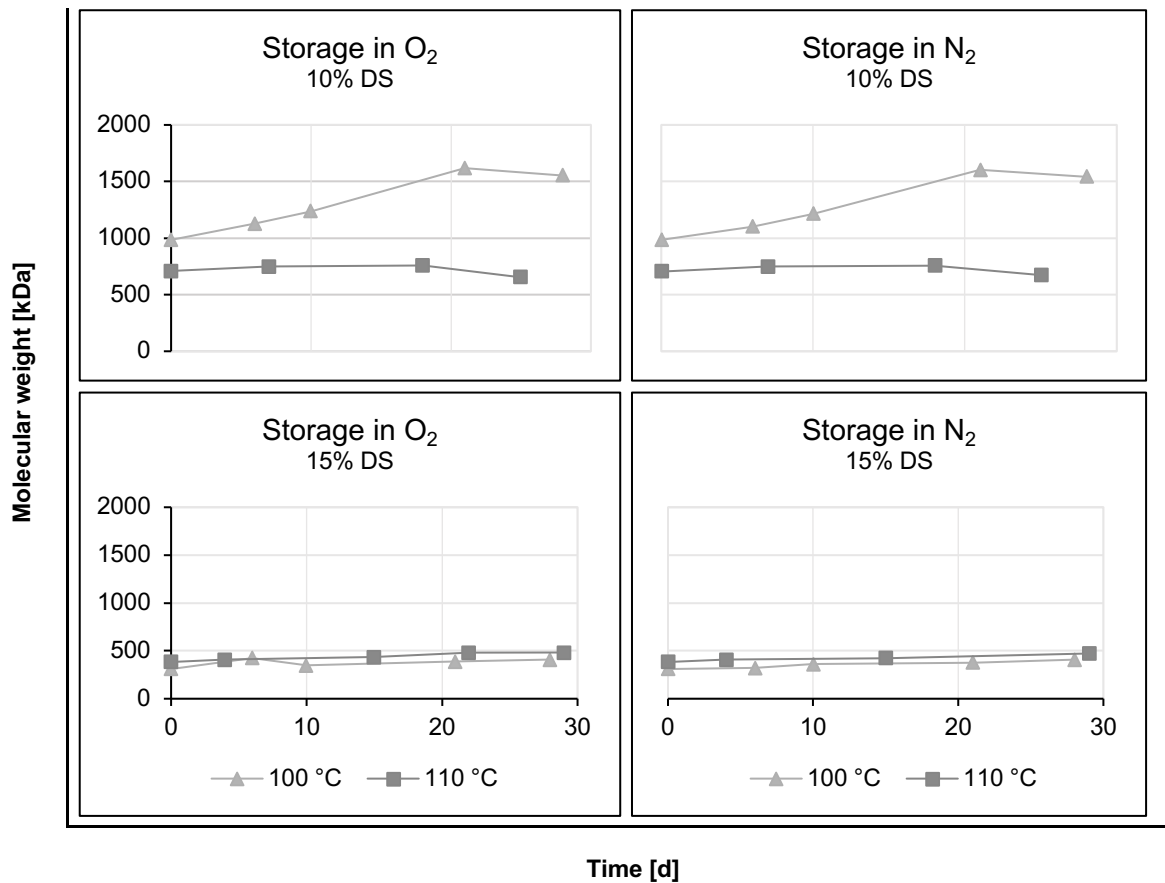
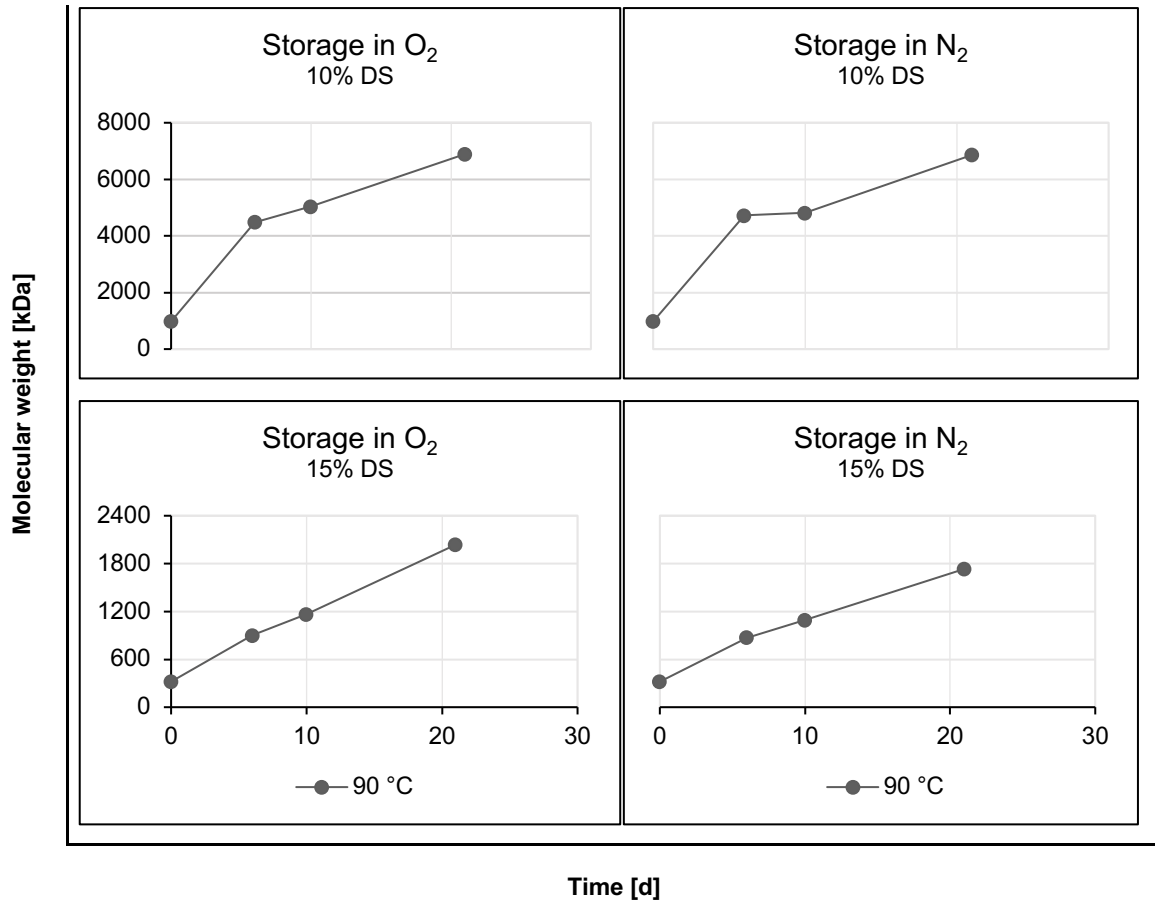


Figure 30: Molecular weights of lignosulfonate polymers stored at different conditions

Figure 30 shows MW results of LS polymers obtained by MALLS detection. As already mentioned above (see figures 28 and 29) storage in contact with air compared to storage in contact with nitrogen shows no significant difference. For 10% (w/v) LS solutions a heat treatment at 110 °C resulted in a rather stable product with variations between 650 and 760 kDa, other than samples incubated at 100 °C, which showed an increase in MW from 980 to 1600 kDa during a storage period of 28 days. Since no residual enzymatic activity was

measured for these samples (see figure 28) the increase in MW might as well be caused by aggregation effects.

15% (w/v) LS solutions treated at 100 °C showed a slight increase from 310-409 kDa. Samples treated at 110 °C varied between 383 and 480 kDa. For both experiments, a trend for a slight increase of MW over time can be observed. Taking the storage time into account, a MW increase of 3.1-3.5 kDa per day can be roughly estimated, suggesting that maximum storage time should be chosen according to requirements regarding product stability.



**Figure 31: Molecular weights of lignosulfonate polymers stored at different conditions**

Figure 31 shows the molecular weights obtained from LS polymers that were incubated at 90 °C. As shown above (figure 23) the enzyme could not be inactivated at 90 °C, which resulted in an increase of MW from 980 to 6900 kDa in the case of the 10% (w/v) LS solution and 320 to 2000 kDa in the case of the 15% (w/v) LS.

## 4 Conclusion and Outlook

During this work the enzyme, *Myceliophthora thermophila* laccase, could be successfully characterized after sufficient purification by laboratory crossflow ultrafiltration and anion exchange chromatography. Size and MW could be determined of the denatured and native enzyme. The MW of MtL in the denatured state obtained with electrophoresis was 95 kDa, while in native state the MW was in a range between 64.6 kDa and 65.8 kDa. However, results gained from MALLS detection are assumed to be most reliable. A PDI of 1.01 shows that the enzyme could be separated completely from impurities by SEC, resulting in a monodisperse sample. Therefore, the result of 64.6 kDa was considered to be most accurate for the native state. Depending on the method, obtained sizes varied between 3.6 nm ( $r_h$ ) and 9.9 nm ( $r_g$ ). Also here, the result obtained from MALLS detection was assumed to be most accurate due to the reasons stated above. Therefore, the size of MtL was stated to be 9.9 nm in radius.

Catalytic constants of MtL were determined at 23 °C with a 50 mM NaPi buffer pH 7.0 by using ABTS as model substrate. Under these conditions the Michaelis constant ( $K_M$ ) was determined to be 832.4  $\mu$ M, while the turnover number ( $k_{cat}$ ) was determined to be 192.4  $s^{-1}$ , resulting in a catalytic efficiency ( $k_{cat}/K_M$ ) of  $2.3 \times 10^5 s^{-1} M^{-1}$ .

In general, the best way to preserve enzymatic activity of MtL is the storage at -80 °C in ultrapure water (see table 17). The least suitable temperature for storage of MtL is +21 °C. Surprisingly, the enzymatic activity of purified MtL that was diluted in ultrapure water (1:100) is better preserved at +4 °C, than -80 °C. However, the purification of the enzyme is economically not feasible in large scale and was done for scientific reasons during this work. Therefore, it should be pointed out that the best storage temperature for the original Novozyme enzyme solution (unpurified undiluted) is at -80 °C.

**Table 17: Summary of storage stability**

Residual activity [%] Temp. [°C]	Unpurified MtL*				Purified MtL**			
	-80	-20	+4	+21	-80	-20	+4	+21
Undiluted	<b>85.7</b>	74.5	28.5	0.9	<b>89.1</b>	84.8	83.9	8.7
Ultrapure water (1:100)	<b>96.4</b>	55.6	66.4	1.5	39.4	28.7	<b>90.7</b>	21.3
50 mM NaPi-buffer (1:100)	62.9	23.4	40.1	14.7	<b>88.3</b>	84.2	84.4	54.4

\*Residual activity of unpurified MtL after 112 days

\*\*Residual activity of purified MtL after 98 days

Values >85% are highlighted

The activity maximum of MtL was determined to be between 60-65 °C with ABTS. However, activities above 70 °C could not be determined due to technical limitations. To confirm this result, it would be necessary to extend the range for activity testing from 70 to 100 °C and

repeat the experiments in triplicates. According to literature, enzymatic activity of MtL increases in a range from 40-90 °C (Ibarra *et al.*, 2006) but also first denaturation effects could be observed at temperatures higher than 70 °C (López-Cruz, Viniegra-González and Hernández-Arana, 2006). Moreover DLS results showed that MtL could not be completely denatured by a 10 min heat treatment at 90, 95 or 99 °C.

LS polymers could be successfully polymerized resulting in an increase of MW. Successful coupling of polymers could also be confirmed by a drop in phenol- and fluorescence content. Enzymatic activity could be monitored indirectly by consumption of dissolved oxygen.

Thermal treatment of polymerized LS showed promising effects regarding enzyme inactivation. Within 20 min incubation time enzymatic activity could be reduced to 0.0-0.5% at 100 °C with a deactivation constant ( $k_d$ ) of 15.9-17.8 h<sup>-1</sup> and a half-life of 0.04 h. At 110 °C no residual activity could be measured after 20 min incubation time, while thermal treatment at 90 °C (40 min) resulted in more than 80% residual activity. Viscosity was decreased by thermal treatment, resulting in a range between 6 and 8 mPas for 10% (w/v) LS incubated at 100 °C (40 min) or 110 °C (20 min). Viscosity of 15% (w/v) LS decreased to 13-33 mPas at 100 or 110 °C. This can be explained by a decrease in MW. For 10% (w/v) LS MW decreased by 32-45% to 660-980 kDa at 100 and 110 °C, while for 15% (w/v) LS the MW decreased by 19-36% to 310-380 kDa. Summarized, it can be stated that inactivation of MtL is possible at 100-110 °C for LS solutions of 10-15% (w/v). Unfortunately, thermal treatments at 100 and 110 °C reduce the MW significantly, although lignin is stated in literature to have a thermal decomposition temperature higher than 280 °C (Brebú and Vasile, 2010). However, the decrease in fluorescence and increase of phenolic content during thermal treatments also indicates a breakage of bonds. Since we missed to get a complete characterization of the raw and diafiltrated material including possible contaminants and interfering substances, we cannot exclude the possibility of substances that could possibly trigger the breakage of bonds by unknown chemical reactions. The complete analysis of the raw material and identification of interfering substances is also highly recommended in order to optimize the purification of spent liquor in a cost effective and target oriented way.

As the main aim of this work was to get a defined and stable end product, heat treated LS polymers were stored in oxygen or nitrogen at 21 °C for 35 days. The nitrogen storage causes the removal of oxygen as electron acceptor and was thereby assumed to be beneficial for product stability. Against our expectations no significant difference could be observed between the LS solution stored in oxygen and nitrogen even for samples where MtL was still active (reference, 90 °C). No residual activity could be observed from LS polymers treated at 100 °C for 40 min and 110 °C for 20 min. Viscosity measurements proved that the material could be

considered as stable with a difference of 2-4 mPas if treated at 100 or 110 °C except the 15% (w/v) solution that was treated at 100 °C (difference of 14 mPas). Viscosity samples were stored at -80 °C prior to measurement. For practical reasons, it was not possible to measure the samples directly after the sampling time points, although this would probably give the most accurate result. Since we did not examine the effect of freezing and thawing LS samples, we have to consider a possible deviation caused by these storing conditions. According to the results obtained from storage stability testings of 15% (w/v) LS solutions, increase of MW shows a positive correlation with time. A MW increase of 3.1-3.5 kDa per day can be roughly estimated, suggesting that product requirements for stability need to be defined in order to choose the maximum possible storage time. However, the enzyme was determined to be completely inactivated. For that reason an increase in MW might be caused by aggregation effects. Further it has to be stated that these experiments were not performed in triplicates, thereby the standard deviation is unknown. In order to improve the quality of the results more measurements would be beneficial.

Summarized it can be said, that LS could be successfully polymerized by laccase and the enzyme could be completely inactivated by thermal treatment at 100 or 110 °C. Compared to reference samples or samples treated at only 90 °C, the LS polymers treated at 100 or 110 °C could be stored for more than 30 days with a reasonable product stability. The outcome of this work could contribute to get further insights into some process aspects of laccase catalyzed polymerizations of LS. However, of course these results can be further improved in several ways. The use of another type of laccase, that denatures at a lower temperature, could help to reduce the decrease of MW during thermal treatment. On the other hand, other laccases might show disadvantages regarding storage stability.

The scientific outcomes gained during this work might also be supplemented by other methods. The content of phenolic hydroxyl groups, for example, could also be determined by nuclear magnetic resonance (NMR) (Zerva *et al.*, 2016).

In our studies, ABTS was used as model substrate for activity assays because it is commonly used for laccase studies and sufficient data can be found for comparison in literature. However, the use of other model substrates for activity assays could be beneficial. Instead of ABTS, 2-methoxyphenol, 2,6-dimethoxyphenol, 3,5-dimethoxy-4-hydroxybenzoic acid, 4-hydroxy-3,5-dimethoxy-cinnamic acid or trans-4-hydroxy-3-methoxy-cinnamic acid, that are more similar to the lignin structure could be used (Schubert *et al.*, 2015).

During this work, purified LS could be successfully polymerized by laccase treatment and a reasonable stable product could be produced after inactivation of the enzyme. In on-going studies, the reproducibility of these results should be determined and improved according to

product requirements. In order to gain experience for the usability of LS polymers as binder in paper coating formulations, the material should be tested in coating trials to replace fossil based latex and thereby improve sustainability in paper production.

## References

- Agrawal, K., Chaturvedi, V. and Verma, P. (2018) 'Fungal laccase discovered but yet undiscovered', *Bioresources and Bioprocessing*. Springer Berlin Heidelberg, 5, pp. 1–12. doi: 10.1186/s40643-018-0190-z.
- Alcalde, M. (2007) 'Laccases: Biological functions, molecular structure and industrial applications', *Industrial Enzymes: Structure, Function and Applications*, pp. 461–476. doi: 10.1007/1-4020-5377-0\_26.
- Aro, T. and Fatehi, P. (2017) 'Production and Application of Lignosulfonates and Sulfonated Lignin', *ChemSusChem*, 10, pp. 1861–1877. doi: 10.1002/cssc.201700082.
- Beckham, G. T. *et al.* (2016) 'Opportunities and challenges in biological lignin valorization', *Current Opinion in Biotechnology*, 42(March), pp. 40–53. doi: 10.1016/j.copbio.2016.02.030.
- Berg, J. M., Tymoczko, J. L. and Stryer, L. (2002) 'The Michaelis-Menten model accounts for the kinetic properties of many enzymes', *Biochemistry*. WH Freeman New York, 5.
- Berg, J. M., Tymoczko, J. L. and Stryer, L. (2013) *Enzyme: Grundlegende Konzepte und Kinetik*, *Biochemiechemie*. doi: 10.1007/978.
- Bhattacharjee, S. (2016) 'DLS and zeta potential - What they are and what they are not?', *Journal of Controlled Release*. Elsevier, 235, pp. 337–351. doi: 10.1016/j.jconrel.2016.06.017.
- Blainski, A., Lopes, G. C. and De Mello, J. C. P. (2013) 'Application and analysis of the folin ciocalteu method for the determination of the total phenolic content from limonium brasiliense L.', *Molecules*, 18, pp. 6852–6865. doi: 10.3390/molecules18066852.
- Brebu, M. and Vasile, C. (2010) 'Thermal Degradation of Lignin – a Review', *Cellulose Chemistry and Technology*, 44, pp. 353–363.
- Cannatelli, M. D. and Ragauskas, A. J. (2016) 'Conversion of lignin into value-added materials and chemicals via laccase-assisted copolymerization', *Applied Microbiology and Biotechnology*. Applied Microbiology and Biotechnology, 100, pp. 8685–8691. doi: 10.1007/s00253-016-7820-1.
- Christopher, L. P., Yao, B. and Ji, Y. (2014) 'Lignin Biodegradation with Laccase-Mediator Systems', *Frontiers in Energy Research*, 2(March), pp. 1–13. doi: 10.3389/fenrg.2014.00012.
- Crestini, C. *et al.* (2010) 'Oxidative strategies in lignin chemistry: A new environmental friendly approach for the functionalisation of lignin and lignocellulosic fibers', *Catalysis Today*. Elsevier, 156, pp. 8–22. doi: 10.1016/j.cattod.2010.03.057.
- Davison, B. H. *et al.* (2006) 'Variation of S/G ratio and lignin content in a Populus family influences the release of xylose by dilute acid hydrolysis', *Applied Biochemistry and Biotechnology*, 129–132, pp. 427–435. doi: 10.1385/ABAB:130:1:427.
- Doran, P. M. (2012) *Bioprocess engineering principles: Second edition*, *Bioprocess Engineering Principles: Second Edition*. doi: 10.1016/S0892-6875(96)90075-8.
- 'Evaluating Lignin-Rich Residues from Biochemical Ethanol Production of Wheat Straw and Olive Tree Pruning by FTIR and 2D-NMR' (2015) *International Journal of Polymer Science*, 2015(March), pp. 1–11. doi: 10.1155/2015/314891.
- Gauglitz, G. (2003) 'Handbook of Spectroscopy'.
- Gillet, S. *et al.* (2017) 'Lignin transformations for high value applications: Towards targeted modifications using green chemistry', *Green Chemistry*, 19, pp. 4200–4233. doi:

## References

10.1039/c7gc01479a.

Gillgren, T., Hedenström, M. and Jönsson, L. J. (2017) 'Comparison of laccase-catalyzed cross-linking of organosolv lignin and lignosulfonates', *International Journal of Biological Macromolecules*. Elsevier B.V., pp. 438–446. doi: 10.1016/j.ijbiomac.2017.07.061.

Gouveia, S. *et al.* (2012) 'Enzymatic polymerisation and effect of fractionation of dissolved lignin from Eucalyptus globulus Kraft liquor', *Bioresource Technology*. Elsevier, 121, pp. 131–138. doi: 10.1016/j.biortech.2012.05.144.

Hilgers, R. *et al.* (2018) 'Laccase/Mediator Systems: Their Reactivity toward Phenolic Lignin Structures', *ACS Sustainable Chemistry and Engineering*, 6(2), pp. 2037–2046. doi: 10.1021/acssuschemeng.7b03451.

Huber, D., Ortner, A., *et al.* (2016) 'Influence of Oxygen and Mediators on Laccase-Catalyzed Polymerization of Lignosulfonate', *ACS Sustainable Chemistry and Engineering*, 4, pp. 5303–5310. doi: 10.1021/acssuschemeng.6b00692.

Huber, D., Pellis, A., *et al.* (2016) 'Polymerization of various lignins via immobilized *Myceliophthora thermophila* Laccase (MtL)', *Polymers*, 8, pp. 1–10. doi: 10.3390/polym8080280.

Hüttermann, A., Mai, C. and Kharazipour, A. (2001) 'Modification of lignin for the production of new compounded materials', *Applied Microbiology and Biotechnology*, 55(4), pp. 387–394. doi: 10.1007/s002530000590.

Ibarra, D. *et al.* (2006) 'Exploring the enzymatic parameters for optimal delignification of eucalypt pulp by laccase-mediator', *Enzyme and Microbial Technology*, 39, pp. 1319–1327. doi: 10.1016/j.enzmictec.2006.03.019.

Jeka, S. *et al.* (2010) 'Principles of a fluorescence phenomenon and its application in medicine', *Reumatologia/Rheumatology*, 48, pp. 257–261.

Jordan, M. A. (1996) 'Bioprocess engineering principles', *Minerals Engineering*. Academic Press, 9(1), pp. 133–135. doi: 10.1016/S0892-6875(96)90075-8.

Karnaouri, A. *et al.* (2014) 'Genomic insights into the fungal lignocellulolytic system of *Myceliophthora thermophila*', *Frontiers in Microbiology*, 5, pp. 1–22. doi: 10.3389/fmicb.2014.00281.

Kenkel, J. (2003) *Analytical Chemistry for Technicians*. 3rd edn.

Kunji, E. R. S. *et al.* (2008) 'Determination of the molecular mass and dimensions of membrane proteins by size exclusion chromatography', *Methods*. Elsevier, 46, pp. 62–72. doi: 10.1016/j.ymeth.2008.10.020.

*Lineweaver-Burk plot* (2019). Available at: [https://en.wikipedia.org/wiki/Lineweaver-Burk\\_plot#/media/File:Lineweaver-Burke\\_plot.svg](https://en.wikipedia.org/wiki/Lineweaver-Burk_plot#/media/File:Lineweaver-Burke_plot.svg) (Accessed: 9 January 2019).

López-Cruz, J. I., Viniestra-González, G. and Hernández-Arana, A. (2006) 'Thermostability of Native and Pegylated *Myceliophthora thermophila* Laccase in Aqueous and Mixed Solvents', *Bioconjugate Chemistry*, 17, pp. 1093–1098. doi: 10.1021/bc0503465.

Lupoi, J. S. *et al.* (2015) 'Recent innovations in analytical methods for the qualitative and quantitative assessment of lignin', *Renewable and Sustainable Energy Reviews*. Elsevier, 49, pp. 871–906. doi: 10.1016/j.rser.2015.04.091.

M. M. Bradford (1976) 'A rapid and sensitive method for the quantitation of microgram quantities of protein utilizing the principle of protein-dye binding', *Analytical biochemistry*, 72, pp. 248–254.

## References

- Mäntele, W. and Deniz, E. (2017) 'UV–VIS absorption spectroscopy: Lambert-Beer reloaded', *Spectrochimica Acta - Part A: Molecular and Biomolecular Spectroscopy*. Elsevier, 173, pp. 965–968. doi: 10.1016/j.saa.2016.09.037.
- Munk, L., Andersen, M. L. and Meyer, A. S. (2018) 'Influence of mediators on laccase catalyzed radical formation in lignin', *Enzyme and Microbial Technology*. Elsevier, 116, pp. 48–56. doi: 10.1016/j.enzmictec.2018.05.009.
- Nugroho Prasetyo, E. *et al.* (2010) 'Polymerization of lignosulfonates by the laccase-HBT (1-hydroxybenzotriazole) system improves dispersibility', *Bioresource Technology*. Elsevier, 101, pp. 5054–5062. doi: 10.1016/j.biortech.2010.01.048.
- Nygaard, M. *et al.* (2017) 'An Efficient Method for Estimating the Hydrodynamic Radius of Disordered Protein Conformations', *Biophysical Journal*. Cell Press, 113, pp. 550–557. doi: 10.1016/J.BPJ.2017.06.042.
- Ortner, A. *et al.* (2015) 'Laccase mediated oxidation of industrial lignins: Is oxygen limiting?', *Process Biochemistry*. Elsevier Ltd, 50(8), pp. 1277–1283. doi: 10.1016/j.procbio.2015.05.003.
- Ortner, A. *et al.* (2018) 'Laccase modified lignosulfonates as novel binder in pigment based paper coating formulations', *Reactive and Functional Polymers*. Elsevier, 123, pp. 20–25. doi: 10.1016/j.reactfunctpolym.2017.12.005.
- Podzimek, S. (2011) *Light Scattering, Size Exclusion Chromatography and Asymmetric Flow Field Flow Fractionation, Powerful Tools for the Characterization of Polymers, Proteins and Nanoparticles*. doi: 10.1002/9780470877975.
- Schubert, M. *et al.* (2015) 'Laccase-catalyzed surface modification of thermo-mechanical pulp (TMP) for the production of wood fiber insulation boards using industrial process water', *PLoS ONE*, 10, pp. 1–15. doi: 10.1371/journal.pone.0128623.
- Strong, P. J. and Claus, H. (2011) 'Laccase: A Review of Its Past and Its Future in Bioremediation', *Critical Reviews in Environmental Science and Technology*. Taylor & Francis, 41, pp. 373–434. doi: 10.1080/10643380902945706.
- Subramanian, A., Prabhakar, V. and Rodriguez-Saona, L. (2011) 'Analytical Methods: Infrared Spectroscopy in Dairy Analysis', in *Encyclopedia of Dairy Sciences: Second Edition*, pp. 115–124. doi: 10.1016/B978-0-12-374407-4.00011-X.
- Uniprot* (2019). Available at: <https://www.uniprot.org/uniprot/G2QG31> (Accessed: 9 January 2019).
- Varanasi, P. *et al.* (2013) 'Survey of renewable chemicals produced from lignocellulosic biomass during ionic liquid pretreatment', *Biotechnology for Biofuels*, 6, pp. 1–9. doi: 10.1186/1754-6834-6-14.
- Zerva, A. *et al.* (2016) 'Bioconversion of biomass-derived phenols catalyzed by *Myceliophthora thermophila* laccase', *Molecules*, 21. doi: 10.3390/molecules21050550.

## Appendix

**Table 18: APPENDIX: MW determination with DLS instrument**

A9 fraction diluted 1:10		
	Radius [nm]	MW-R [kDa]
M2	3.3	56.7
M4	3.8	75.1
M5	3.5	62.1
M6	3.8	74.4
M7	4.1	93.2
M8	3.3	56.5
M9	3.7	71.2
M10	3.0	42.4
M11	3.4	59.0
M12	3.6	69.3
M13	3.5	63.5
<b>Mean</b>	<b>3.6</b>	<b>65.8</b>
<b>STD</b>	<b>0.3</b>	<b>13.2</b>

**Table 19: APPENDIX: MW determination with MALLS**

Diluted to 1 mg/mL	Mw [Da]	Mw [kDa]	PDI Mw/Mn	rz [nm]
	64100	64.1	1.01	9.3
	64500	64.5	1.01	8.8
	65100	65.1	1.01	11.5
<b>Mean</b>	<b>64567</b>	<b>64.6</b>		<b>9.9</b>
<b>STD</b>	<b>503.32</b>	<b>0.5</b>		<b>1.4</b>

**Table 20: APPENDIX: Theoretical MW computation with ProtParam**

<p><b>Uniprot:</b>  <a href="https://www.uniprot.org/uniprot/G2QG31">https://www.uniprot.org/uniprot/G2QG31</a></p> <p><b>Protparam:</b>  <a href="https://web.expasy.org/cgi-bin/protparam/protparam1?G2QG31@noft@">https://web.expasy.org/cgi-bin/protparam/protparam1?G2QG31@noft@</a></p> <p><b>ProtParam</b>  <u>G2QG31_MYCTT (G2QG31)</u></p> <p>Extracellular laccase, lcc1  Myceliophthora thermophila (strain ATCC 42464 / BCRC 31852 / DSM 1799)  (Sporotrichum thermophile).  The computation has been carried out on the complete sequence (<b>616</b> amino acids).</p> <hr/> <p><b>Number of amino acids:</b> 616</p> <p><b>Molecular weight:</b> 67579.55</p> <p><b>Theoretical pI:</b> 5.28</p> <p>Extinction coefficients are in units of <math>M^{-1} cm^{-1}</math>, at 280 nm measured in water.</p> <p><b>Ext. coefficient 128145</b>  Abs 0.1% (=1 g/l) 1.896, assuming all pairs of Cys residues form cystines</p> <p>Ext. coefficient 127770  Abs 0.1% (=1 g/l) 1.891, assuming all Cys residues are reduced</p> <p>The instability index (II) is computed to be 33.94  This classifies the protein as stable.</p> <div style="border: 1px dashed black; padding: 5px; margin: 10px 0;"> <p>Signal peptide: MKSFISAATL LVGILTPSVA A</p> </div> <p><b>Signal peptide</b></p> <p><b>User-provided sequence:</b>            10    20  MKSFISAATL LVGILTPSVA A</p> <hr/> <p><b>Number of amino acids:</b> 21</p> <p><b>Molecular weight:</b> 2090.55</p> <p><b>Theoretical pI:</b> 8.50</p> <p><b>Extinction coefficients:</b></p> <p>As there are no Trp, Tyr or Cys in the region considered, your protein should not be visible by UV spectrophotometry.  The instability index (II) is computed to be 19.78. This classifies the protein as stable.</p>
---

Appendix

**Table 21: APPENDIX: Bradford protein concentration of purified MtL**

	Conc. [mg/mL]
	8.8
	8.6
	8.6
<b>Mean</b>	<b>8.7</b>
<b>STD</b>	<b>0.1</b>

**Table 22: APPENDIX: BSA standard calibration**

Conc. [g/L]	MW Abs.	- Blank
0.25	0.80	0.46
0.2	0.70	0.37
0.1	0.50	0.17
0.05	0.40	0.07
0.025	0.34	0.01

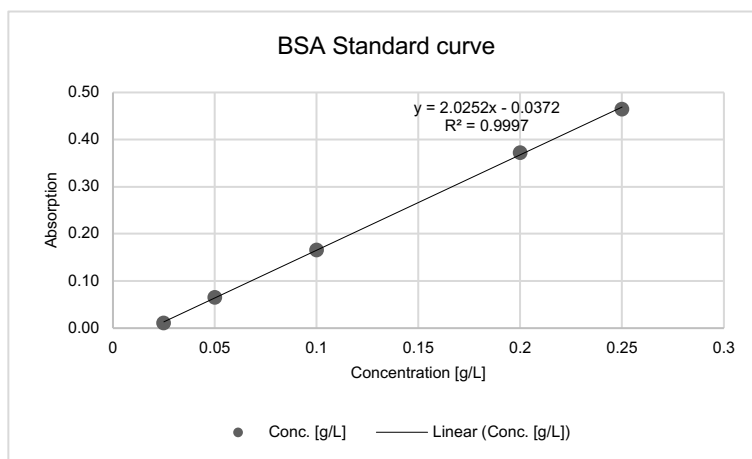


**Figure 32: APPENDIX: BSA standard calibration curve**

**Table 23: APPENDIX: Michaelis-Menten plot**

ABTS Stock [mM]	ABTS [mM]	MW Activity [U/mL]	STD [U/mL]
40	9.09	1341.35	145.08
30	6.82	1257.68	190.37
20	4.55	1200.56	127.93
15	3.41	1189.88	68.01
10	2.27	1165.91	119.05
5	1.14	929.57	82.89
2.5	0.57	655.78	37.16
1	0.23	338.76	17.05
0.75	0.17	269.12	15.30
0.5	0.11	185.15	8.78
0.25	0.06	98.56	5.52
0.1	0.02	40.15	2.81

## Appendix

**Table 24: APPENDIX: Lineweaver–Burk plot**

1/S	1/V
0.11	0.000745519
0.15	0.000795117
0.22	0.000832946
0.29	0.000840421
0.44	0.000857701
0.88	0.001075763
1.76	0.0015249
4.40	0.002951919
5.87	0.003715777
8.80	0.005401022
17.60	0.010145723

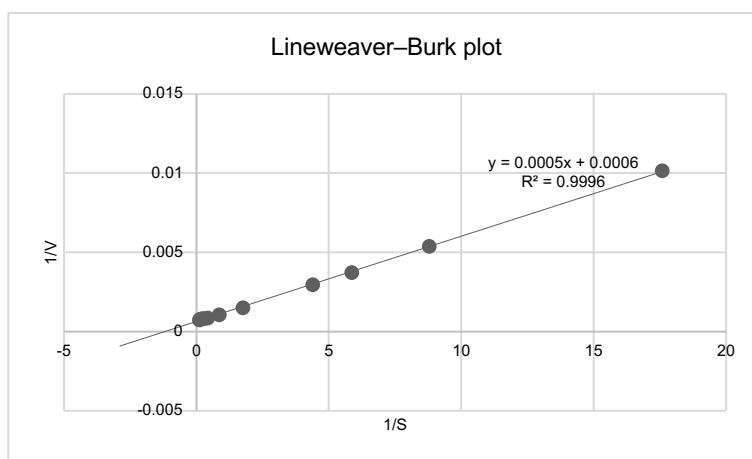


**Figure 33: APPENDIX: Double reciprocal Lineweaver Burk plot of purified Mtl**

Appendix

**Table 25: APPENDIX: Storage stability data of unpurified MtL**

	Temp. [°C]	Time [days]	0	1	2	3	7	21	31	35	56	70	84	98	112	
Undiluted unpurified MtL	-80	Activity [U/mL]	1275.7	1191.5	1172.2	1245.6	1167.1	1097.6	1069.6	1040.5	1104.2	1076.8	1053.4	1175.2	1093.7	
		Activity [%]	100.0	93.4	91.9	97.6	91.5	86.0	83.8	81.6	86.6	84.4	82.6		85.7	
	-20	Activity [U/mL]	1275.7	1177.7	1167.8	1181.5	1117.5	1058.5	892.0	1025.1	923.3	945.5	951.3	959.7	950.3	
		Activity [%]	100.0	92.3	91.5	92.6	87.6	83.0		80.4	72.4	74.1	74.6	75.2	74.5	
	4	Activity [U/mL]	1275.7		1118.2	1017.8	970.3	883.7	833.7	780.5	751.9	798.9	683.7	532.9	363.0	
		Activity [%]	100.0		87.7	79.8	76.1	69.3	65.3	61.2	58.9		53.6	41.8	28.5	
	21	Activity [U/mL]	1275.7	1233.2	1166.0	1111.5	1133.3	1107.7	907.6	1024.6	922.1	819.8	529.7	150.1	11.9	
		Activity [%]	100.0	96.7	91.4	87.1	88.8	86.8		80.3	72.3	64.3	41.5	11.8	0.9	
	Unpurified MtL 1:100 diluted in 50mM Na <sub>2</sub> HPO <sub>4</sub>	-80	Activity [U/mL]	1275.7	1102.0	1148.5	1108.2	1054.4	837.1	832.0	828.0	708.2	878.4	780.5	784.3	802.7
			Activity [%]	100.0	86.4	90.0	86.9	82.7	65.6	65.2	64.9	55.5		61.2	61.5	62.9
		-20	Activity [U/mL]	1275.7	849.7	888.3	851.8	819.2	519.6	398.3	428.0	377.4	374.6	345.3	372.4	298.6
			Activity [%]	100.0		69.6	66.8	64.2	40.7	31.2	33.6	29.6	29.4	27.1	29.2	23.4
4		Activity [U/mL]	1275.7	1238.6	1258.1	1221.6	1191.2	911.2	715.4	776.7	725.7	880.0	715.1	724.9	625.9	
		Activity [%]	100.0	97.1	98.6	95.8	93.4	71.4		60.9	56.9		56.1	56.8	49.1	
21		Activity [U/mL]	1275.7	1192.6	1115.3	1105.0	880.7	701.9	533.4	457.9	389.2	515.2	365.9	293.8	188.0	
		Activity [%]	100.0	93.5	87.4	86.6	69.0	55.0	41.8	35.9	30.5		28.7	23.0	14.7	
Unpurified MtL 1:100 diluted in ultrapure water		-80	Activity [U/mL]	1539.4	1539.4	1522.0	1482.2	1509.0	1480.6	1466.4	1530.7	1463.0	1488.8	1501.5	1438.9	1484.5
			Activity [%]	100.0	100.0	98.9	96.3	98.0	96.2	95.3		95.0	96.7	97.5	93.5	96.4
		-20	Activity [U/mL]	1575.4	1575.4	1535.3	1438.4	1352.2	1245.9	1072.5	1049.1	1009.7	1014.5	1018.5	850.6	876.1
			Activity [%]	100.0	100.0	97.5	91.3	85.8	79.1	68.1	66.6	64.1	64.4	64.6		55.6
	4	Activity [U/mL]	1571.3	1571.3	1550.2	1472.7	1471.7	1239.3	1197.8	1176.7	1154.4	1119.7	1125.1	1105.4	1042.8	
		Activity [%]	100.0	100.0	98.7	93.7	93.7	78.9	76.2	74.9	73.5	71.3	71.6	70.4	66.4	
	21	Activity [U/mL]	1497.1	1497.1	1453.5	1302.6	1085.3	805.6	595.9	538.3	259.8	125.8	59.6	35.3	22.8	
		Activity [%]	100.0	100.0	97.1	87.0	72.5	53.8	39.8	36.0	17.4	8.4	4.0	2.4	1.5	

Appendix

**Table 26: APPENDIX: Storage stability data of purified MtL**

	Temp. [°C]	Time [days]	0	1	2	7	16	21	42	56	70	84	98
Undiluted purified MtL	-80	Activity [U/mL]	758.5	748.0	732.5	740.7	702.1	723.5	720.6	641.7	689.5	716.9	675.9
		Activity [%]	100.0	98.6	96.6	97.7	92.6	95.4	95.0	84.6	90.9	94.5	89.1
	-20	Activity [U/mL]	758.5	704.7	699.4	720.7	661.2	624.1	671.9	622.5	647.0	668.3	642.9
		Activity [%]	100.0	92.9	92.2	95.0	87.2	82.3	88.6	82.1	85.3	88.1	84.8
	4	Activity [U/mL]	758.5	758.5	698.9	728.0	700.6	750.5	691.9	646.4	611.5	657.1	636.0
		Activity [%]	100.0	100.0	92.1	96.0	92.4	98.9	91.2	85.2	80.6	86.6	83.9
21	Activity [U/mL]	758.5	758.8	719.4	663.0	543.8	527.2	361.9	232.4	155.7	101.0	65.9	
	Activity [%]	100.0	100.0	94.8	87.4	71.7	69.5	47.7	30.6	20.5	13.3	8.7	
Purified MtL 1:100 diluted in 50mM Na <sub>2</sub> HPO <sub>4</sub>	-80	Activity [U/mL]	758.5	544.7	503.9	416.5	397.2	469.1	262.0	240.8	318.8	282.7	298.8
		Activity [%]	100.0	71.8	66.4	54.9	52.4		34.5	31.7	42.0	37.3	39.4
	-20	Activity [U/mL]	758.5	233.2	209.5	217.7	201.3	208.4	207.5	213.1	246.9	201.1	217.3
		Activity [%]	100.0	30.8	27.6	28.7	26.5	27.5	27.4	28.1	32.5	26.5	28.7
	4	Activity [U/mL]	758.5	779.9	753.0	742.7	723.9	759.0	674.5	649.7	651.3	677.3	687.7
		Activity [%]	100.0	102.8	99.3	97.9	95.4	100.1	88.9	85.7	85.9	89.3	90.7
21	Activity [U/mL]	758.5	784.1	726.2	714.1	625.8	518.2	436.0	280.3	258.3	149.2	161.2	
	Activity [%]	100.0	103.4	95.8	94.1	82.5	68.3	57.5	37.0	34.1	19.7	21.3	
Purified MtL 1:100 diluted in ultrapure water	-80	Activity [U/mL]	758.5	631.6	705.6	605.1	666.4	675.2	621.3	627.0	706.9	665.8	669.7
		Activity [%]	100.0		93.0		87.9		81.9	82.7	93.2	87.8	88.3
	-20	Activity [U/mL]	758.5	657.6	716.1	668.0	666.9	524.0	634.2	596.2	645.8	607.4	638.7
		Activity [%]	100.0		94.4	88.1	87.9		83.6	78.6	85.1	80.1	84.2
	4	Activity [U/mL]	844.6	844.6	852.1	883.2	850.7	858.6	831.3	727.1	763.4	744.6	712.6
		Activity [%]	100.0	100.0	100.9	104.6	100.7	101.7	98.4	86.1	90.4	88.2	84.4
21	Activity [U/mL]	857.0	857.0	848.3	846.8	813.9	680.7	667.1	550.8	533.5	491.0	466.4	
	Activity [%]	100.0	100.0	99.0	98.8	95.0		77.8	64.3	62.2	57.3	54.4	

**Table 27: APPENDIX: Temperatur optimum**

Unpurified MtL			Purified MtL		
Temp [°C]	Activity [U/mL]	STD [U/mL]	Temp [°C]	Activity [U/ml]	STD [U/mL]
35	2061.5	22.7	35	1728.9	31.6
40	2396.0	6.9	40	2109.7	38.0
45	2605.8	15.6	45	2425.4	30.3
50	3153.4	104.9	50	2741.7	50.3
55	3395.5	98.0	55	3124.6	56.7
60	4922.3	129.7	60	3253.3	67.6
65	3832.9	68.3	65	3472.9	114.6
70	4110.1	195.3	70	3459.5	183.1

**Table 28: APPENDIX: Effect of high temperatures**

90 °C			95 °C			99 °C		
Measur.	Time [s]	D10 radius [nm]	Measur.	Time [s]	D10 radius [nm]	Measur.	Time [s]	D10 radius [nm]
M5	320	6.8	M3	81	6.0	M1	0	7.7
M6	460	5.5	M4	120	5.8	M6	200	6.3
M7	550	4.5	M6	200	5.2	M10	370	4.7
M8	590	4.2	M11	410	4.3	/	/	/
M10	670	3.8	/	/	/	/	/	/

**Table 29: APPENDIX: Increase of molecular weight during polymerization**

Mean values 10%							
Timepoint	Time [min]	Mw [Da]	Mw [kDa]	STD	PDI Mw/Mn	rz [nm]	
TP0	0	185700	185.7	1.4	1.89	15.1	
TP1	30	418950	419.0	76.3	2.30	22.6	
TP2	60	723100	723.1	39.0	2.59	28.8	
Mean values 15%							
Timepoint	Time [min]	Mw [Da]	Mw [kDa]	STD	PDI Mw/Mn	rz [nm]	
TP0	0	218800	218.8	34.5	1.84	16.7	
TP1	30	398150	398.2	177.3	2.22	22.8	

**Table 30: APPENDIX: Fluorescence during polymerization and after thermal treatment**

Lignosulfonate	Fluor. [RFU]	STD [RFU]	Fluor. [x 1000 RFU]
0 min	5725000.0	41.5	5725.0
20 min	2356666.7	29.0	2356.7
40 min	1838333.3	10.0	1838.3
60 min	1601666.7	5.0	1601.7
80 min	1715000.0	6.1	1715.0
90 °C	1623333.3	4.2	1623.3
100 °C	2040000.0	14.0	2040.0
110 °C	2131667.0	7.0	2131.7

Appendix

**Table 31: APPENDIX: Phenol content during polymerization and after thermal treatment**

Lignosulfonate	Phenol cont. [mmol/L]	STD [mmol/L]
0 min	78.6	1.7
20 min	68.8	0.6
40 min	59.4	0.1
60 min	58.2	0.5
80 min	56.4	0.3
90 °C	73.1	0.8
100 °C	69.6	0.3
110 °C	79.2	0.8

**Table 32: APPENDIX: Activity during thermal treatment**

Activity [%]		10%				
Temp [°C]	Time [min]	0	10	20	30	40
90 °C		100.0	99.7	92.9	80.1	81.7
100 °C		100.0	40.7	0.5	0	0
110 °C		100.0	/	0	/	/
Activity [%]		15%				
Temp [°C]	Time [min]	0	10	20	30	40
90 °C		100.0	114.4	102.7	94.0	81.8
100 °C		100.0	5.1	0	0.2	0.8
110 °C		100.0	/	0	/	/

**Table 33: APPENDIX: Thermal stability**

10%					
Temp [°C]	A <sub>0</sub>	A <sub>r</sub>	Time [h]	kd [h <sup>-1</sup> ]	t <sub>0.5</sub> [h]
100	462.9	2.4	0.3	15.8	0.04
110	169.2	0.0	0.3	n.a.	n.a.
15%					
Temp [°C]	A <sub>0</sub>	A <sub>r</sub>	Time [h]	kd [h <sup>-1</sup> ]	t <sub>0.5</sub> [h]
100	232.0	11.9	0.2	17.8	0.04
110	123.6	0.0	0.3	n.a.	n.a.

**Table 34: APPENDIX: Viscosity during thermal treatment**

Viscosity [mPas]		10%				
Temp [°C]	Time [min]	0	10	20	30	40
90 °C		73.6	19.1	18.5	19.5	12.4
100 °C		45.8	15.8	8.6	7.9	7.9
110 °C		93.5	/	6.2	/	/

Viscosity [mPas]		15%				
Temp [°C]	Time [min]	0	10	20	30	40
90 °C		22.5	11.7	10.6	10.1	11.3
100 °C		20.6	10.6	10.2	14.7	13.0
110 °C		117.6	/	32.7	/	/

**Table 35: APPENDIX: Molecular weight during thermal treatment**

		10%					
	Timepoint	Time [min]	Mw [Da]	Mw [kDa]	PDI	Mw/Mn	rz [nm]
90 °C	TP0	0	1456000	1456	2.87		41.5
	TP1	10	1229000	1229	2.76		37.5
	TP2	20	1124000	1124	2.75		37.0
	TP3	30	1038000	1038	2.65		34.4
	TP4	40	977500	978	2.61		33.3

		10%					
	Timepoint	Time [min]	Mw [Da]	Mw [kDa]	PDI	Mw/Mn	rz [nm]
100 °C	TP0	0	1456000	1456	2.87		41.5
	TP1	10	1337700	1338	2.86		40.0
	TP2	20	1137700	1138	2.72		36.6
	TP3	30	1050800	1051	2.67		34.9
	TP4	40	984400	984	2.62		33.9

		10%					
	Timepoint	Time [min]	Mw [Da]	Mw [kDa]	PDI	Mw/Mn	rz [nm]
110 °C	TP0	0	1201900	1202	2.76		38.4
	TP1	20	657800	658	2.36		26.6

		15%					
	Timepoint	Time [min]	Mw [Da]	Mw [kDa]	PDI	Mw/Mn	rz [nm]
90 °C	TP0	0	381600	382	2.22		21.5
	TP1	10	339500	340	2.20		21.6
	TP2	20	328400	328	2.18		21.2
	TP3	30	326900	327	2.20		21.5
	TP4	40	319900	320	2.19		21.4

		15%					
	Timepoint	Time [min]	Mw [Da]	Mw [kDa]	PDI	Mw/Mn	rz [nm]
100 °C	TP0	0	411000	411	2.39		24.2
	TP1	10	347700	348	2.21		21.7
	TP2	20	325400	325	2.16		21.2
	TP3	30	323100	323	2.21		22.6
	TP4	40	310000	310	2.03		21.3

		15%					
	Timepoint	Time [min]	Mw [Da]	Mw [kDa]	PDI	Mw/Mn	rz [nm]
110 °C	TP0	0	603600	604	2.58		28.8
	TP1	20	383400	383	2.19		23.1

Appendix

**Table 36: APPENDIX: Activity during storage**

Activity [%]		10% LS storage in O <sub>2</sub>				
Temp [°C]	Time [days]	0	6	10	21	28
	Ref.	100.0	94.7	94.3	35.0	X
	90 °C	81.7	104.0	113.6	115.0	X
	100 °C	0	0	0	0	0
Temp [°C]	Time [days]	0	7	18	25	35
	110 °C	0	2.3	0	0	0.3
Activity [%]		10% LS storage in N <sub>2</sub>				
Temp [°C]	Time [days]	0	6	10	21	28
	Ref.	100.0	103.5	87.4	X	X
	90 °C	81.7	100.1	105.5	101.3	X
	100 °C	0	0	0	0	0
Temp [°C]	Time [days]	0	7	18	25	35
	110 °C	0	0	0	0	0
Activity [%]		15% LS storage in O <sub>2</sub>				
Temp [°C]	Time [days]	0	6	10	21	28
	Ref.	100.0			69.3	X
	90 °C	81.8	116.0	114.4		X
	100 °C	0.7	0	0	0	0
Temp [°C]	Time [days]	0	7	18	25	35
	110 °C	0	0	0	0	0
Activity [%]		15% LS storage in N <sub>2</sub>				
Temp [°C]	Time [days]	0	6	10	21	28
	Ref.	100.0			107.5	X
	90 °C	81.8	106.7	107.5	117.6	X
	100 °C	0.7	5.9	0	3.3	0
Temp [°C]	Time [days]	0	7	18	25	35
	110 °C	0	6.4	0	0	0

Appendix

**Table 37: APPENDIX: Viscosity during storage**

Viscosity [mPas]		10% LS storage in O <sub>2</sub>					
Temp [°C]	Time [days]	0	6	10	21	28	
100 °C			7.9	10.6	9.4	10.9	12.0
Temp [°C]	Time [days]	0	7	18	25	35	
110 °C			6.2	6.8	6.5	6.6	6.4
Viscosity [mPas]		10% LS storage in N <sub>2</sub>					
Temp [°C]	Time [days]	0	6	10	21	28	
100 °C			7.9	8.7	9.3	10.5	11.0
Temp [°C]	Time [days]	0	7	18	25	35	
110 °C			6.2	8.0	7.1	6.4	6.0
Viscosity [mPas]		15% LS storage in O <sub>2</sub>					
Temp [°C]	Time [days]	0	6	10	21	28	
100 °C			13.0	15.9	15.8	14.4	13.7
Temp [°C]	Time [days]	0	7	18	25	35	
110 °C			11.2	11.4	11.6	11.9	
Viscosity [mPas]		15% LS storage in N <sub>2</sub>					
Temp [°C]	Time [days]	0	6	10	21	28	
100 °C			13.0	12.9	11.6	25.8	21.8
Temp [°C]	Time [days]	0	7	18	25	35	
110 °C			11.0	10.9	8.9	11.1	

**Table 38: APPENDIX: MW during storage**

		10% LS storage in O <sub>2</sub>					
	Timepoint	Days [d]	Mw [Da]	Mw [kDa]	PDI	Mw/Mn	rz [nm]
90 °C	TP0	0	977500	978	2.61		33.3
	TP1	6	4490200	4490	2.75		63.7
	TP2	10	5040300	5040	2.60		69.1
	TP3	21	6890800	6891	2.90		73.1
100 °C	Timepoint	Days [d]	Mw [Da]	Mw [kDa]	PDI	Mw/Mn	rz [nm]
	TP0	0	984400	984	2.62		33.9
	TP1	6	1127700	1128	2.73		36.7
	TP2	10	1235900	1236	2.92		38.6
	TP3	21	1618200	1618	3.05		45.6
110 °C	TP4	28	1553400	1553	2.86		44.2
	Timepoint	Days [d]	Mw [Da]	Mw [kDa]	PDI	Mw/Mn	rz [nm]
	TP0	0	708300	708	2.41		28.8
	TP1	7	748100	748	2.48		29.4
	TP2	18	758100	758	2.53		30.2
	TP3	25	653500	654	2.20		26.6

## Appendix

Continuation of table 38

10% LS storage in N <sub>2</sub>							
	Timepoint	Days [d]	Mw [Da]	Mw [kDa]	PDI	Mw/Mn	rz [nm]
90 °C	TP0	0	977500	978	2.61		33.3
	TP1	6	4719900	4720	2.73		67.6
	TP2	10	4816300	4816	2.60		63.5
	TP3	21	6860800	6861	2.20		73.1
	Timepoint	Days [d]	Mw [Da]	Mw [kDa]	PDI	Mw/Mn	rz [nm]
100 °C	TP0	0	984400	984	2.62		33.9
	TP1	6	1102200	1102	2.70		35.6
	TP2	10	1214100	1214	2.90		37.6
	TP3	21	1603500	1604	3.07		44.6
	TP4	28	1543300	1543	2.88		42.9
	Timepoint	Days [d]	Mw [Da]	Mw [kDa]	PDI	Mw/Mn	rz [nm]
110 °C	TP0	0	706400	706	2.40		28.4
	TP1	7	747300	747	2.48		29.5
	TP2	18	756300	756	2.53		30.0
	TP3	25	673100	673	2.30		27.3
15% LS storage in O <sub>2</sub>							
	Timepoint	Days [d]	Mw [Da]	Mw [kDa]	PDI	Mw/Mn	rz [nm]
90 °C	TP0	0	319900	320	2.19		21.4
	TP1	6	899400	899	2.89		38.8
	TP2	10	1165500	1166	3.05		43.5
	TP3	21	2036400	2036	3.08		50.3
	Timepoint	Days [d]	Mw [Da]	Mw [kDa]	PDI	Mw/Mn	rz [nm]
100 °C	TP0	0	310000	310	2.03		21.3
	TP1	6	424200	424	2.19		22.7
	TP2	10	346600	347	2.24		25.4
	TP3	21	388700	389	2.36		25.0
	TP4	28	408500	409	2.38		25.2
	Timepoint	Days [d]	Mw [Da]	Mw [kDa]	PDI	Mw/Mn	rz [nm]
110 °C	TP0	0	383400	383	2.19		23.1
	TP1	4	406800	407	2.23		24.1
	TP2	15	434100	434	2.31		24.5
	TP3	22	481300	481	2.23		24.9
	TP4	29	480400	480	2.40		25.4

Appendix

**Continuation of table 38**

		15% LS storage in N <sub>2</sub>					
	Timepoint	Days [d]	Mw [Da]	Mw [kDa]	PDI	Mw/Mn	rz [nm]
90 °C	TP0	0	319900	320	2.19		21.4
	TP1	6	869800	870	2.86		38.3
	TP2	10	1091100	1091	3.04		42.1
	TP3	21	1733900	1734	3.03		50.1
	Timepoint	Days [d]	Mw [Da]	Mw [kDa]	PDI	Mw/Mn	rz [nm]
100 °C	TP0	0	310000	310	2.03		21.3
	TP1	6	321600	322	2.16		22.3
	TP2	10	360300	360	2.21		24.5
	TP3	21	378600	379	2.33		24.6
	TP4	28	408300	408	2.35		25.4
	Timepoint	Days [d]	Mw [Da]	Mw [kDa]	PDI	Mw/Mn	rz [nm]
110 °C	TP0	0	383400	383	2.19		23.1
	TP1	4	407400	407	2.23		24.0
	TP2	15	424400	424	2.28		23.8
	TP3	22	X	X	X		X
	TP4	29	472500	473	2.35		25.1